Treatment Assessment of Radiotherapy using MR Functional Quantitative Imaging: Promises and Challenges

Zheng Chang, Ph.D.
Department of Radiation Oncology, Duke University, NC

Outline

- Introduction of MR quantitative imaging for treatment assessment
- Review of diffusion imaging, DCE/DSC imaging…
- Treatment assessment using diffusion MRI
- Treatment assessment using DCE-MRI
- Developments of MR quantitative imaging for treatment assessment
- Challenges and future directions

Outline

- Introduction of MR quantitative imaging for treatment assessment
- Review of diffusion imaging, DCE/DSC imaging…
- Treatment assessment using diffusion MRI
- Treatment assessment using DCE-MRI
- Developments of MR quantitative imaging for treatment assessment
- Challenges and future directions

Introduction

Recent developments in MRI have substantially improved its performance

Anatomic ➡ Angiographic ➡ Physiologic ➡ Interventions

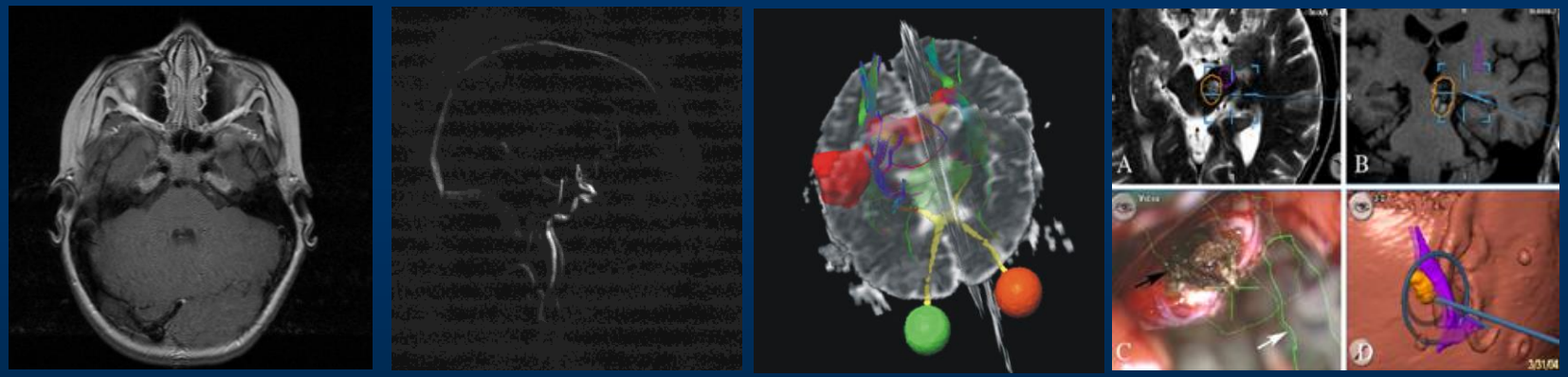

Making it a potentially powerful tool for not only diagnosis but also therapy.

Introduction

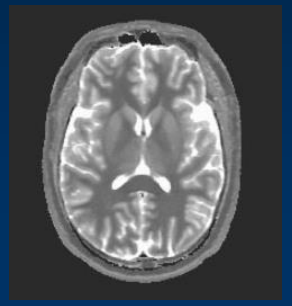

T1 mapping

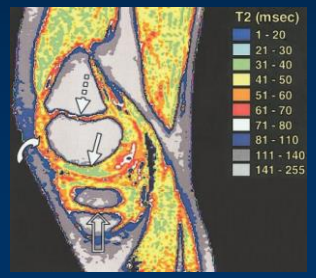

T2 mapping

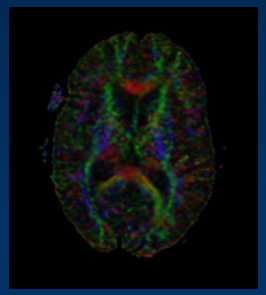

FA map

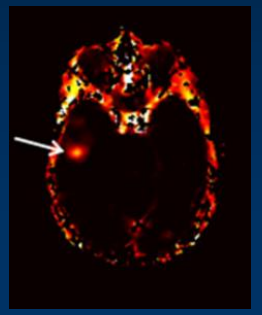

K^{trans} map

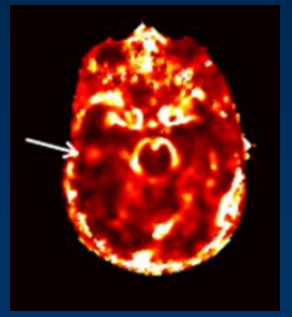

F_B map

Zhu,et al, MRM 2005

Chang,et al, TCRT 2014

Wang,et al, MRM 2015

Wang,et al, TCRT 2016

Dardzinski,et al, Pediatric Imaging 2015

Various MR quantitative functional techniques including, but not limited to, DWI, DTI, MRS and DCE/DSC imaging, have been investigated to assess therapeutic outcome in radiotherapy

Treatment Simulation

Treatment Planning

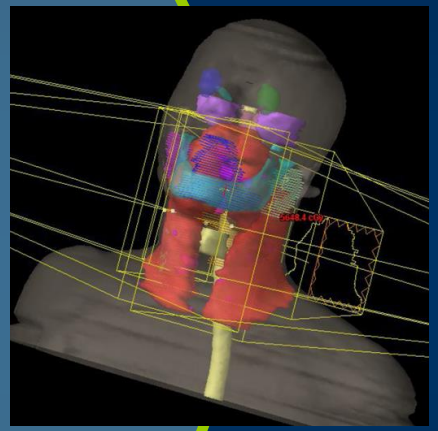

Image-Guided Treatment

?

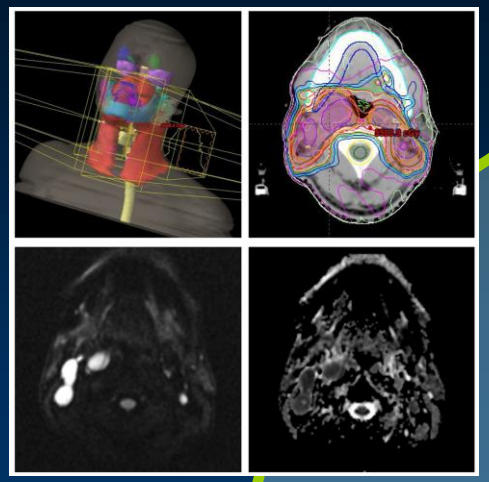

Treatment Simulation

Treatment Planning

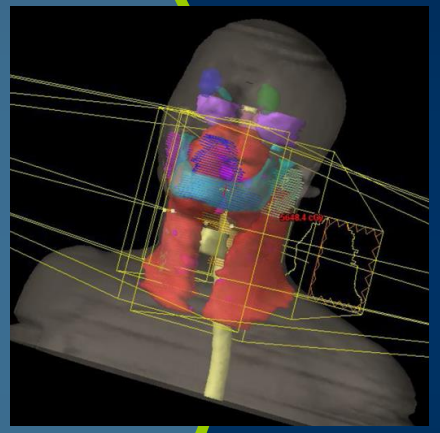

Image-Guided Treatment

Treatment Assessment

Outline

- Introduction of MR quantitative imaging for treatment assessment
- Review of diffusion imaging, DCE/DSC imaging…
- Treatment assessment using diffusion MRI
- Treatment assessment using DCE-MRI
- Developments of MR quantitative imaging for treatment assessment
- Challenges and future directions

Diffusion Imaging

Diffusion imaging techniques are used to determine the rate and principle direction of thermal (Brownian) motion of protons

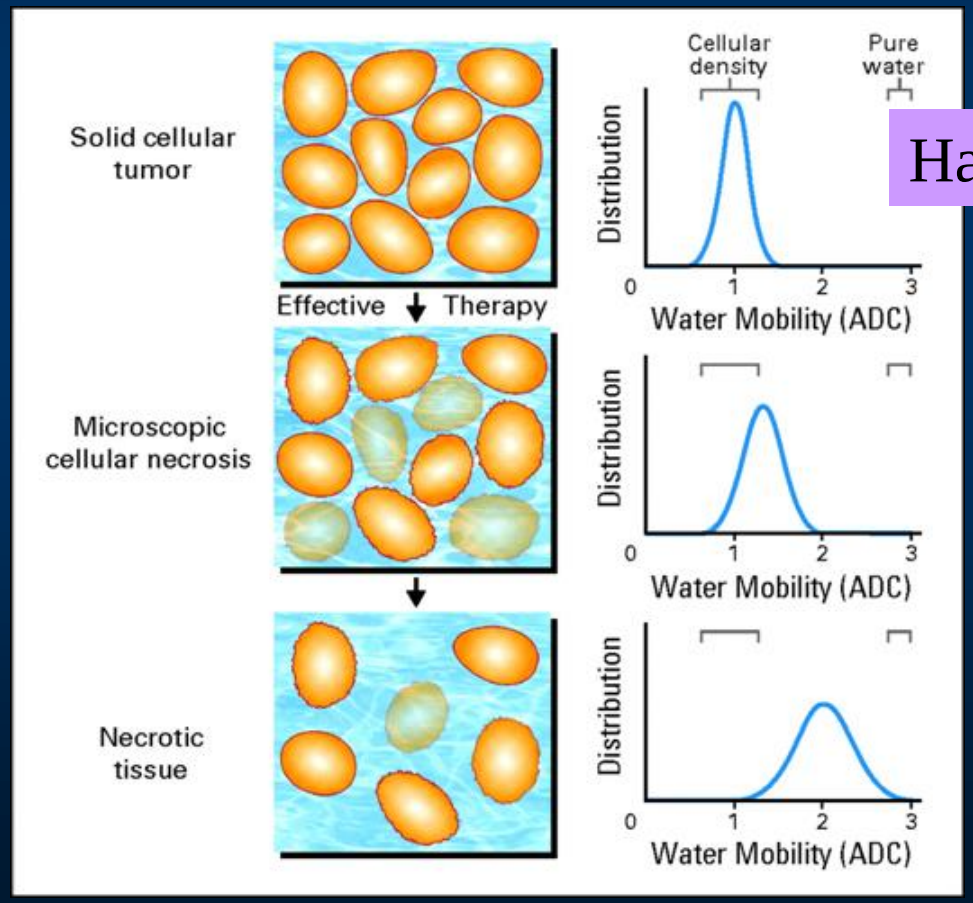

Hamstra,et al, JCO 2007

Diffusion affected by intra-cellular and extra-cellular architecture

Diffusion-Weighting Gradients

Tissue A

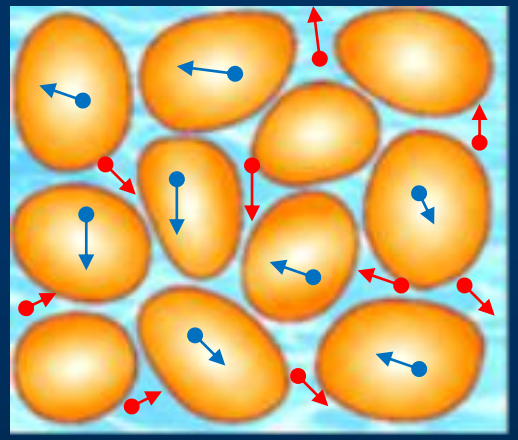

Restricted Diffusion
Bright Contrast

Tissue B

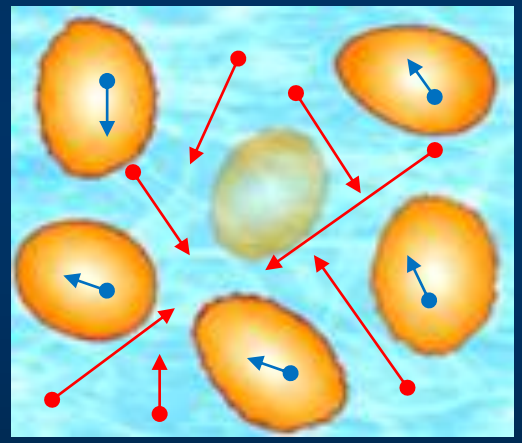

Freely Diffusion
Dark Contrast

Diffusion-Weighting Gradients

Diffusion-weighting gradient is often referred to as bipolar gradient (or Stejskal-Tanner gradient)

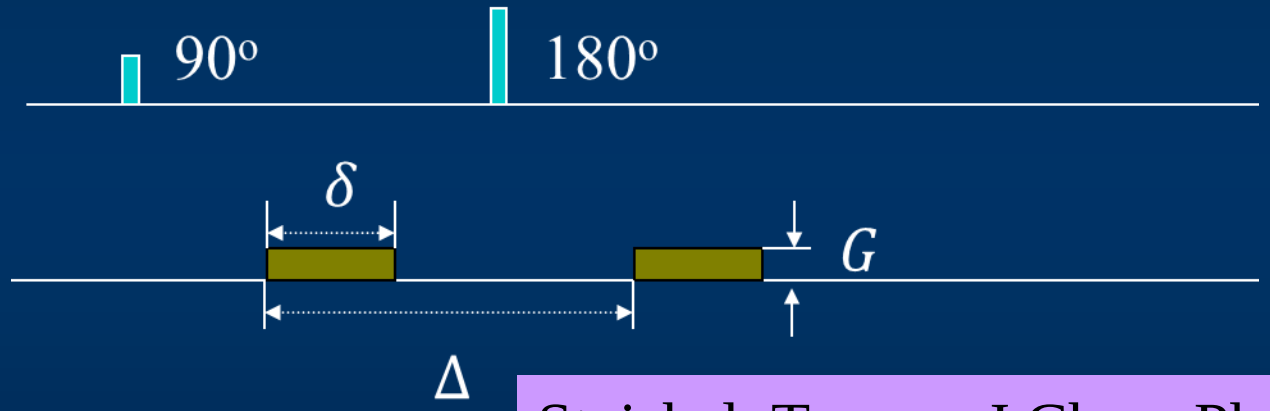

Stejskal, Tanner. J Chem Physics, 1965

Spin Echo: 90° RF, first gradient lobe, 180° RF, second gradient lobe

Diffusion-Weighting Gradients

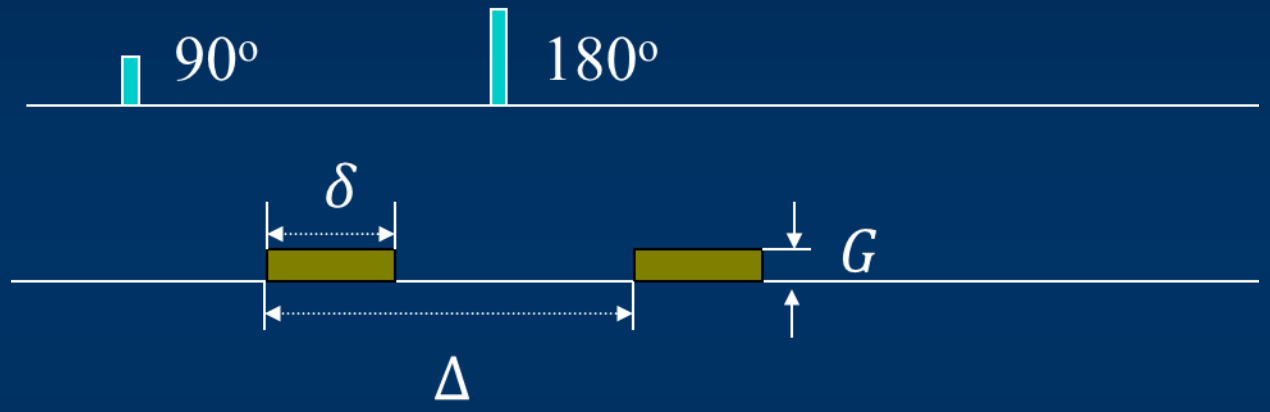

b-factor for rectangular pulse of spin echo

$$b = \gamma^2 G^2 \delta^2 (\Delta - \delta/3)$$

$$\rightarrow \quad \frac{S}{S_0} = \exp(-bD)$$

High b-Value Diffusion

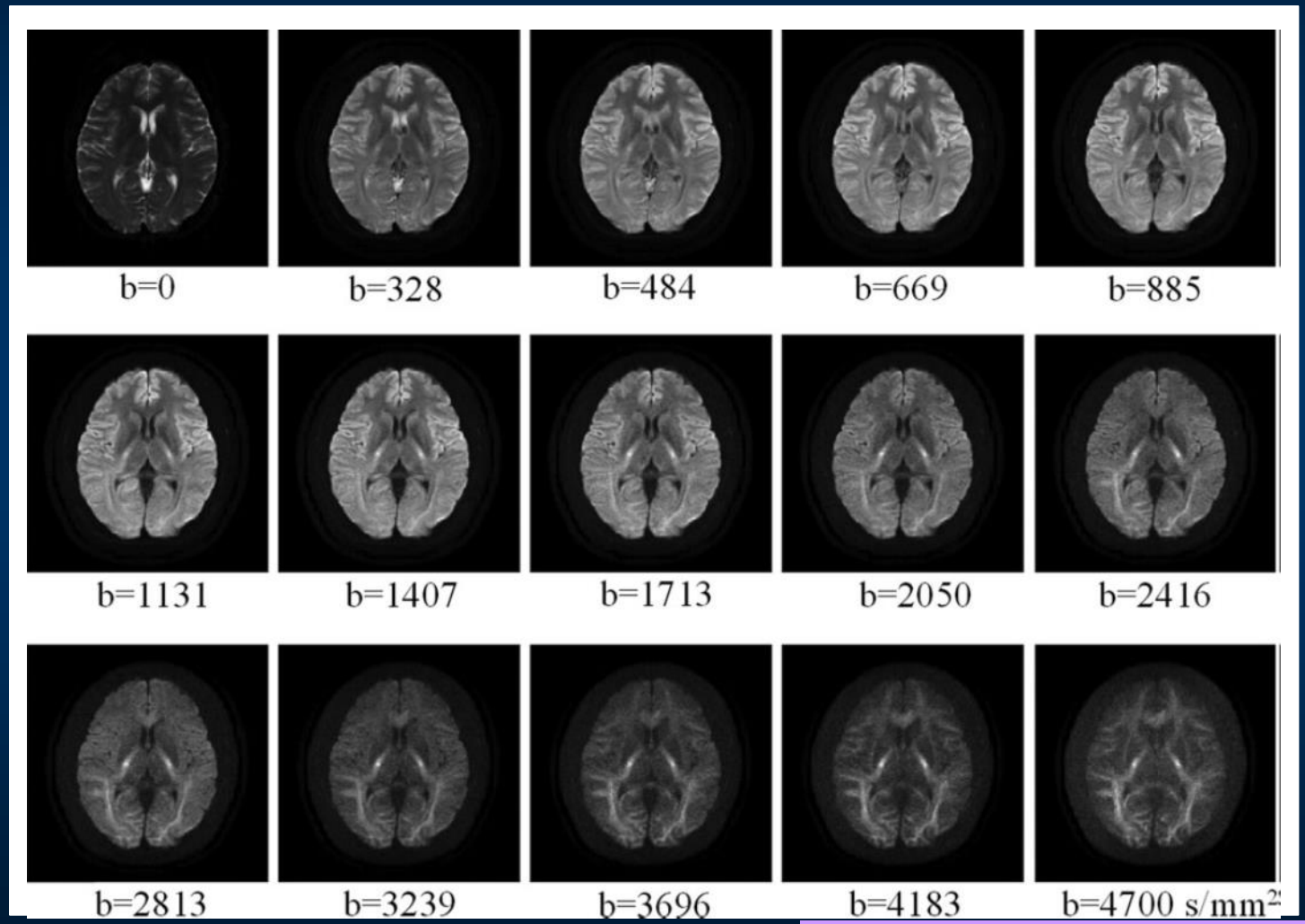

Zhou, et al. MRM, 2010

Diffusion Tensor Imaging

Diffusion is truly a three-dimensional process. Hence, molecular mobility in tissues may not be the same in all directions.

- Diffusion can be described by a tensor, with min. 7 acquisitions.
- The diffusion tensor can be an ellipsoidal approximation

$$\bar{\bar{D}} = \begin{bmatrix} D_{xx} & D_{xy} & D_{xz} \\ D_{yx} & D_{yy} & D_{yz} \\ D_{zx} & D_{zy} & D_{zz} \end{bmatrix}$$

$$\bar{\bar{D}} = \bar{E}^{-1} \begin{bmatrix} \boldsymbol{\lambda_1} & \mathbf{0} & \mathbf{0} \\ \mathbf{0} & \boldsymbol{\lambda_2} & \mathbf{0} \\ \mathbf{0} & \mathbf{0} & \boldsymbol{\lambda_3} \end{bmatrix} \bar{E}$$

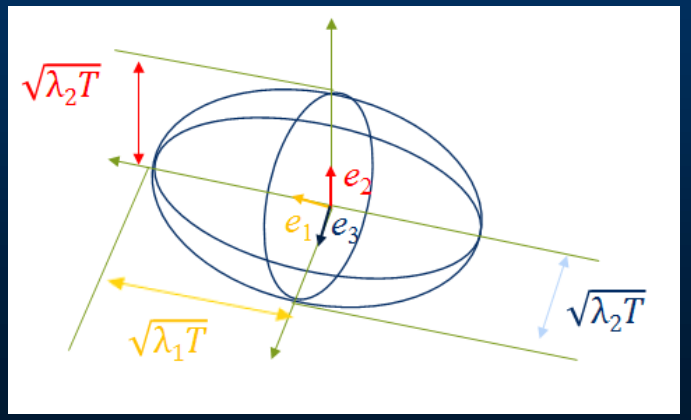

D Le Bihan, et al. JMRI, 2001

Diffusion Tensor Imaging

Diffusion is truly a three-dimensional process. Hence, molecular mobility in tissues may not be the same in all directions.

- Diffusion can be described by a tensor, with min. 7 acquisitions.

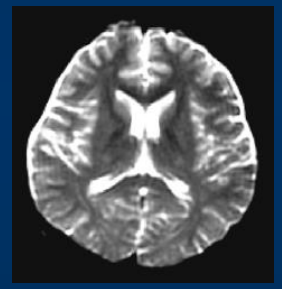

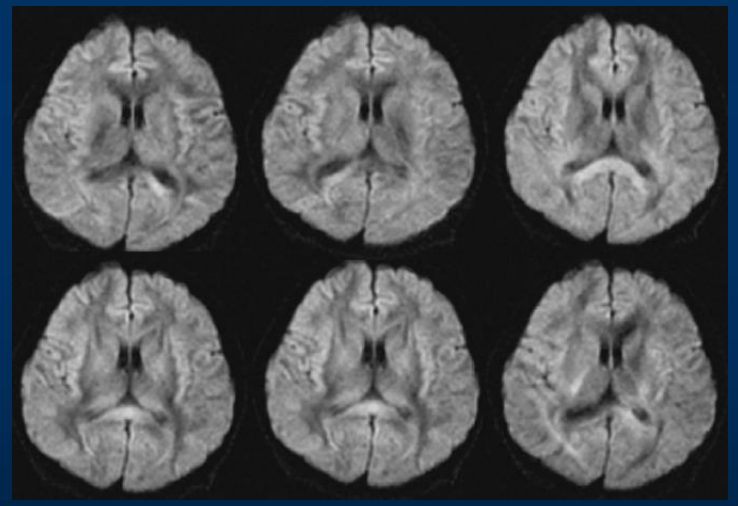

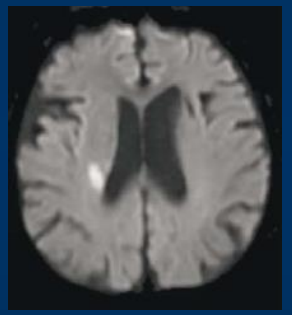

Mean Diffusivity <D>Map

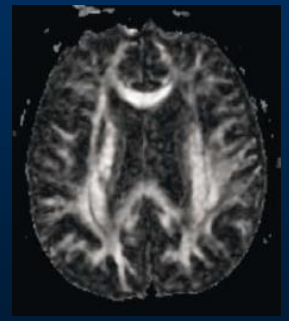

FA map

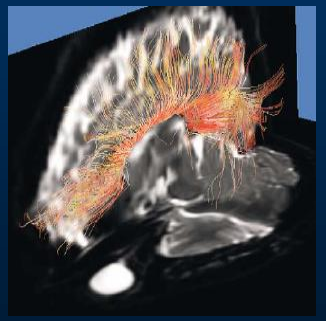

Fiber Tractography

D Le Bihan, et al. JMRI, 2001

Y. Masutani et al. EJR, 2003

Outline

- Introduction of MR quantitative imaging for treatment assessment
- Review of diffusion imaging, DCE/DSC imaging…
- Treatment assessment using diffusion MRI
- Treatment assessment using DCE-MRI
- Developments of MR quantitative imaging for treatment assessment
- Challenges and future directions

Angiogenesis

- Angiogenesis is a complex process critical to the growth and metastasis of malignant tumors.
- Tumor growth beyond 1–2 mm in solid tissues cannot occur without vascular support.
- Early detection of such changes would allow assessment of the therapeutic outcome of anti-vascular agents and aid in diagnosis.

J. Folkman Eur J Cancer 1996

Detection of Angiogenesis

Current methods of assessing angiogenesis can be considered as either direct or indirect.

- direct method: microvascular density counting with immunostaining (most frequently used)

  - invasive and no functional information

- indirect method: indirect biomarkers of angiogenesis detected by imaging such as MRI using contrast agent (e.g. Gd)

  - Non-invasive and provide functional information

J.A. d'Arcy RadioGraphics 2006

DCE and DSC MRI

Table 1
Comparison of the T2*- and T1-weighted Dynamic Contrast-enhanced MR Imaging Techniques

Parameter	T2*-weighted Imaging	T1-weighted Imaging
Change in tissue signal intensity	Darkening	Enhancement
Duration of effect	Seconds	Minutes
Period of optimal data acquisition	Subsecond	2–25 sec
Magnitude of effect	Small	Larger
Optimal dose of contrast medium	≥0.2 mmol/kg	0.1–0.2 mmol/kg
Quantification methods used	Relative more than absolute	Relative and absolute
Physiologic properties measured	Perfusion, blood volume	Transendothelial permeability, capillary surface area, lesion leakage space
Kinetic parameters derived	Blood volume and flow, transit time	Transfer and rate constants, leakage space
Pathologic correlates	Tumor grade, microvessel density	Microvessel density, vascular endothelial growth factor
Clinical MR imaging applications	Characterization of breast, liver, and brain lesions; noninvasive grading of brain tumors; directing biopsy of brain tumors; determination of prognosis for brain tumors; monitoring treatment (eg, radiation	Lesion detection and characterization; improving accuracy of tumor staging; prediction of response to treatment; monitoring response to treatment; allowing novel therapies, including antiangiogenic drugs; detection of tumor relapse

J.A. d'Arcy RadioGraphics 2006

DCE-MRI

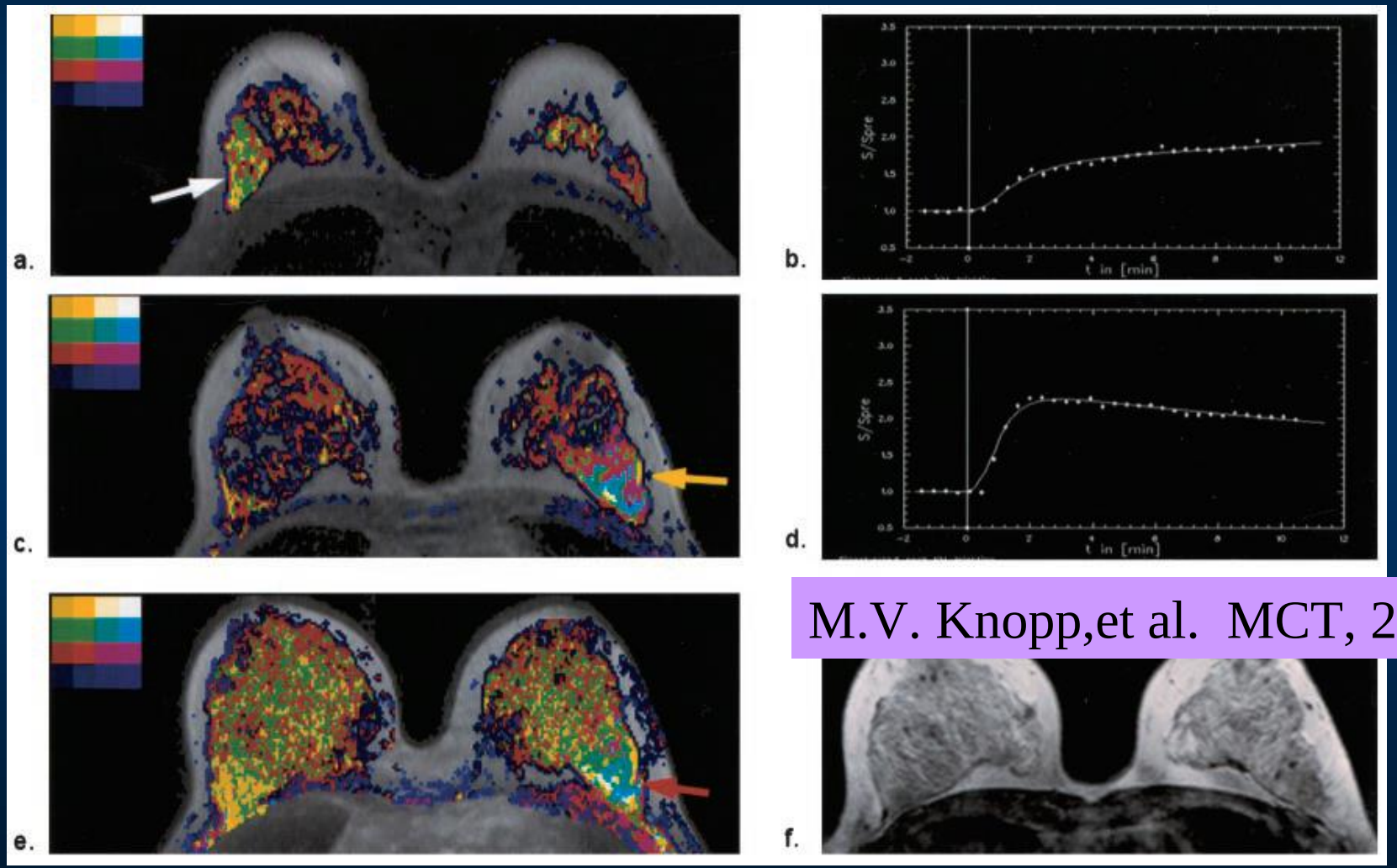

M.V. Knopp,et al. MCT, 2003

DCE-MRI : Pharmacokinetic Model

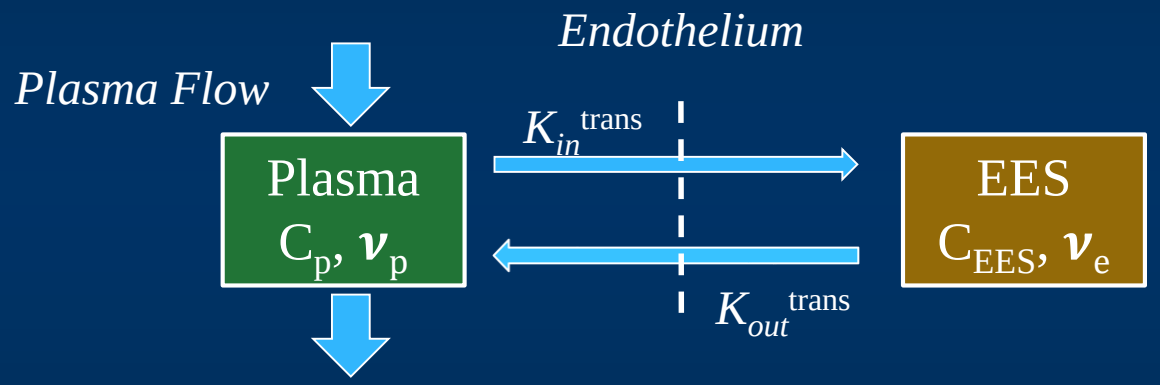

P.S. Tofts, et al. JMRI, 1997

Pharmacokinetic Model

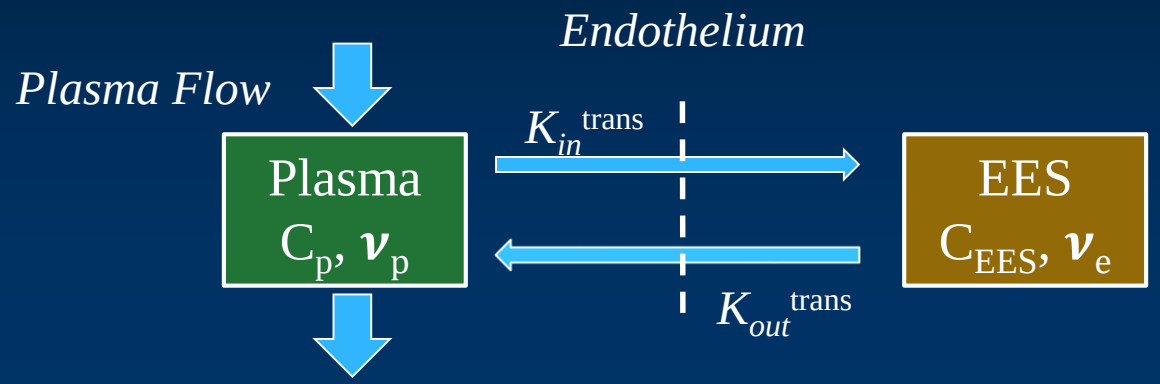

$$C(t) = CEE_S(t) + \nu_p C_p(t)$$

C(t) = [Gd] in tissue measured

$$C(t) = Kin^{trans} \int_0^t Cp(t')e^{-Ko_{uttr}{}^{an}/\nu_e\,(t-t')}\mathrm{d}t' + \nu_p C_p(t)$$

P.S. Tofts, et al. JMRI, 1997

Pharmacokinetic Model

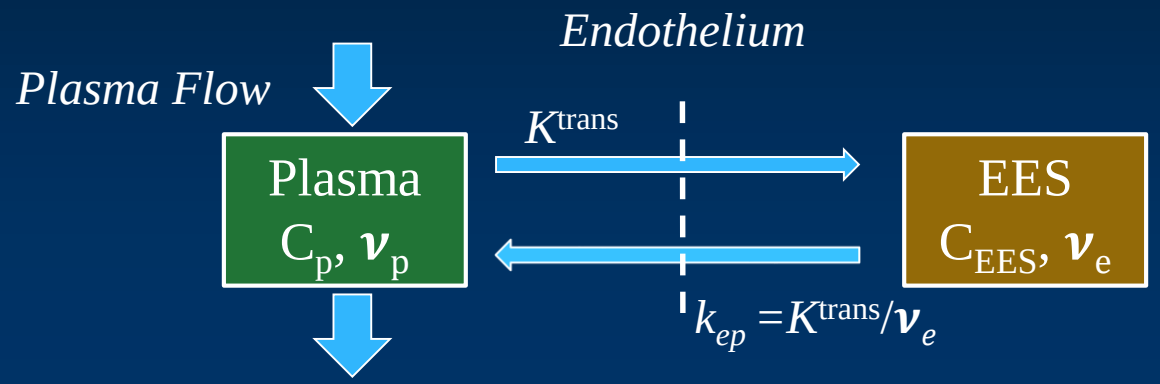

$$C(t) = Kin^{trans} \int_0^t Cp(t')e^{-Ko_{uttr}{}^{an}/\nu_e (t-t')}\mathrm{d}t' + \nu_p C_p(t)$$

Assume small plasma volume $\nu_p = 0$ and $K_{in}{}^{Trans} = K_{out}{}^{Trans}$

$$\Rightarrow \quad C(t) = Ktr^{ans} \int_0^t Cp(t')e^{-ke_p(t-t')}\mathrm{d}t'$$

DCE-MRI Analysis

- Qualitative
  - Uptake curves

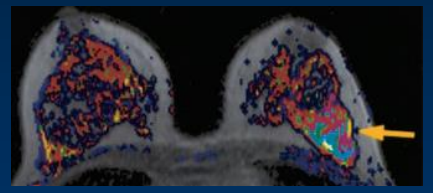

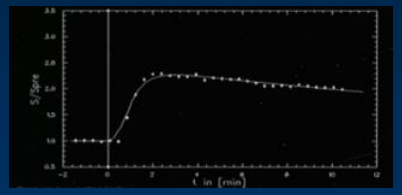

- Semi-quantitative
  - Area under the curve (AUC)

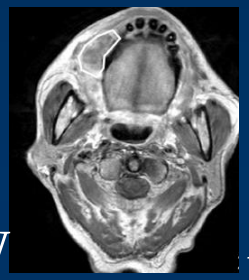

T1W

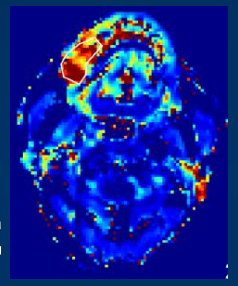

AUC

- Quantitative
  - Tracer-kinetic modeling (K^{trans}, V_B, F_B, etc)

M.V. Knopp,et al. MCT, 2003

A.D. King, et al, PLOS, 2015

Wang,et al, TCRT 2016

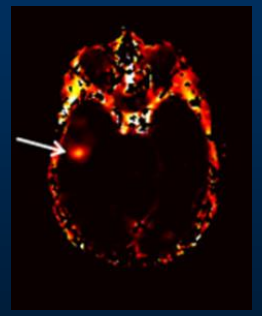

K^{trans} map

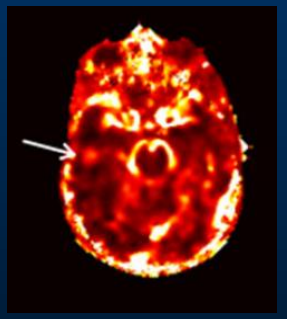

F_B map

Outline

- Introduction of MR quantitative imaging for treatment assessment
- Review of diffusion imaging, DCE/DSC imaging…
- Treatment assessment using diffusion MRI
  - Assessment of tumor response
  - Assessment of radiation-induced normal tissue damage
- Treatment assessment using DCE-MRI
- Developments of MR quantitative imaging for treatment assessment
- Challenges and future directions

Assessment using Diffusion MRI –Brian tumors

- For malignant glioma, the radiologic response (RR) method using 3D measurements of tumor volume - association with survival.
- One disadvantage of volume measures is the time for changes to occur, with 8 to 10 weeks necessary to assess response.
- Diffusion imaging (DTI) could be used to investigate the feasibility of detection of early response…
- A brain study of 60 patients with high-grade glioma, with gross tumor treated to a final median dose of 70 Gy in 6-7 weeks. Diffusion imaging with a single-shot, spin-echo, echo-planar imaging (EPI) sequence. Scanned 1 week before and 1, 3, and 10 weeks after the start of radiation.

D. A. Hamstra, JCO, 2008

Assessment using Diffusion

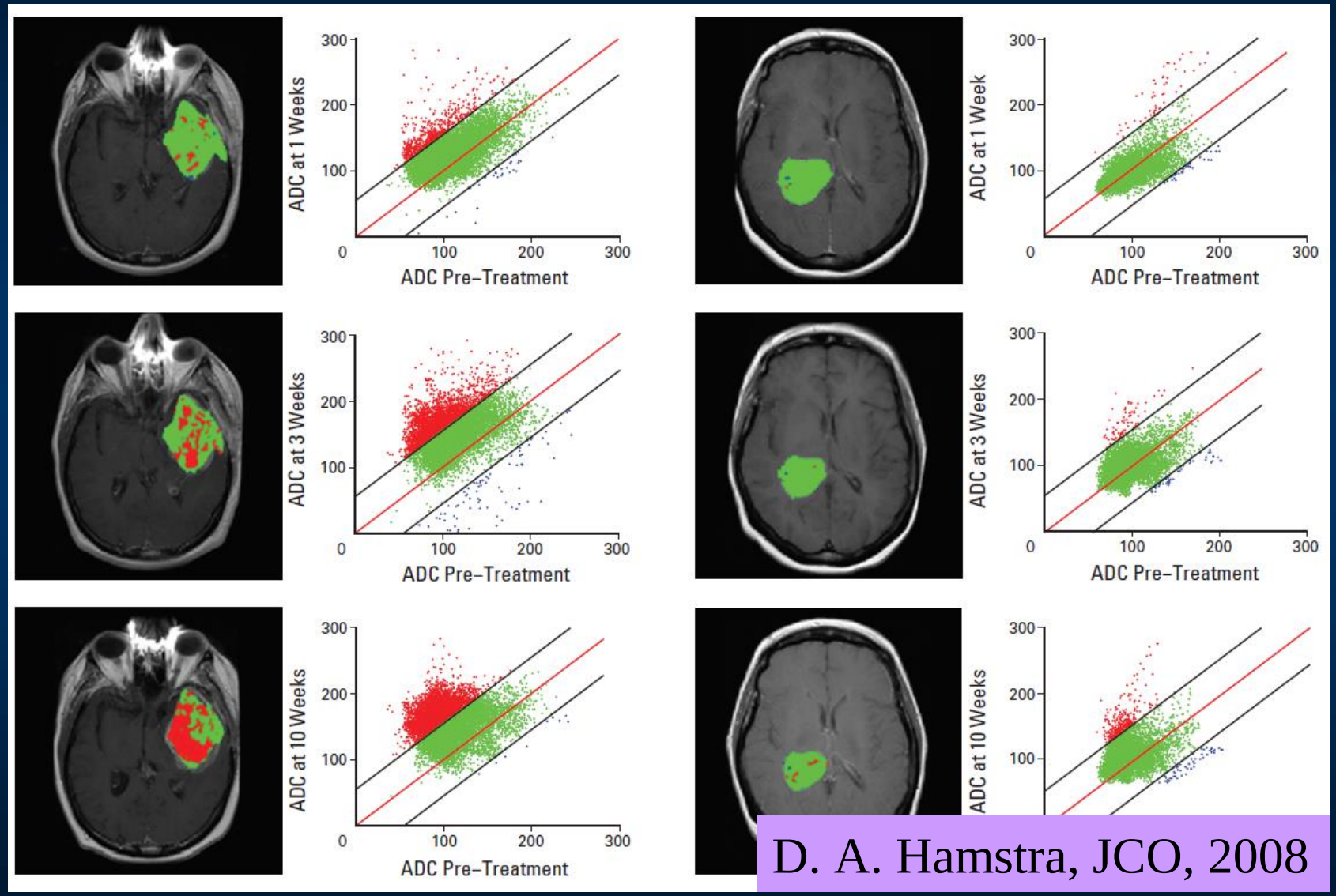

D. A. Hamstra, JCO, 2008

Early Assessed; Better OS Functional diffusion map (fDM): Red –ADC Increased

Assessment using Diffusion MRI –Brian tumors

- For malignant glioma, the radiologic response (RR) method using 3D measurements of tumor volume - association with survival.
- One disadvantage of volume measures is the time for changes to occur, with 8 to 10 weeks necessary to assess response.
- Increased diffusion of water molecules (measured as an increase in the apparent diffusion coefficient (ADC)) occurs shortly after a successful treatment, and correlates with the breakdown of cellular membranes and reduction in cell density that both precede changes in tumor size.

D. A. Hamstra, JCO, 2008

Outline

- Introduction of MR quantitative imaging for treatment assessment
- Review of diffusion imaging, DCE/DSC imaging…
- Treatment assessment using diffusion MRI
  - Assessment of tumor response
  - Assessment of radiation-induced normal tissue damage
- Treatment assessment using DCE-MRI
- Developments of MR quantitative imaging for treatment assessment
- Challenges and future directions

Assessment using Diffusion MRI –White Matter Damage

- Stereotactic radiosurgery (SRS) has been an effective treatment for the management of brain metastases, acoustic neuromas and other brain diseases.
- Few data are available regarding radiation induced white matter (WM) damage by SRS.
- Diffusion tensor imaging (DTI) was used to investigate WM changes following SRS …
- A study of 15 patients with recurrent unifocal malignant gliomas, treated with concurrent SRS/BVZ treatment, with radiation dose of from 18Gy to 25Gy. Scanned 1-4 days prior to SRS and 7 days and two months after SRS treatment

Chang Z, et al., Technol Cancer Res Treat, 2014.

Assessment using Diffusion MRI –White Matter Damage

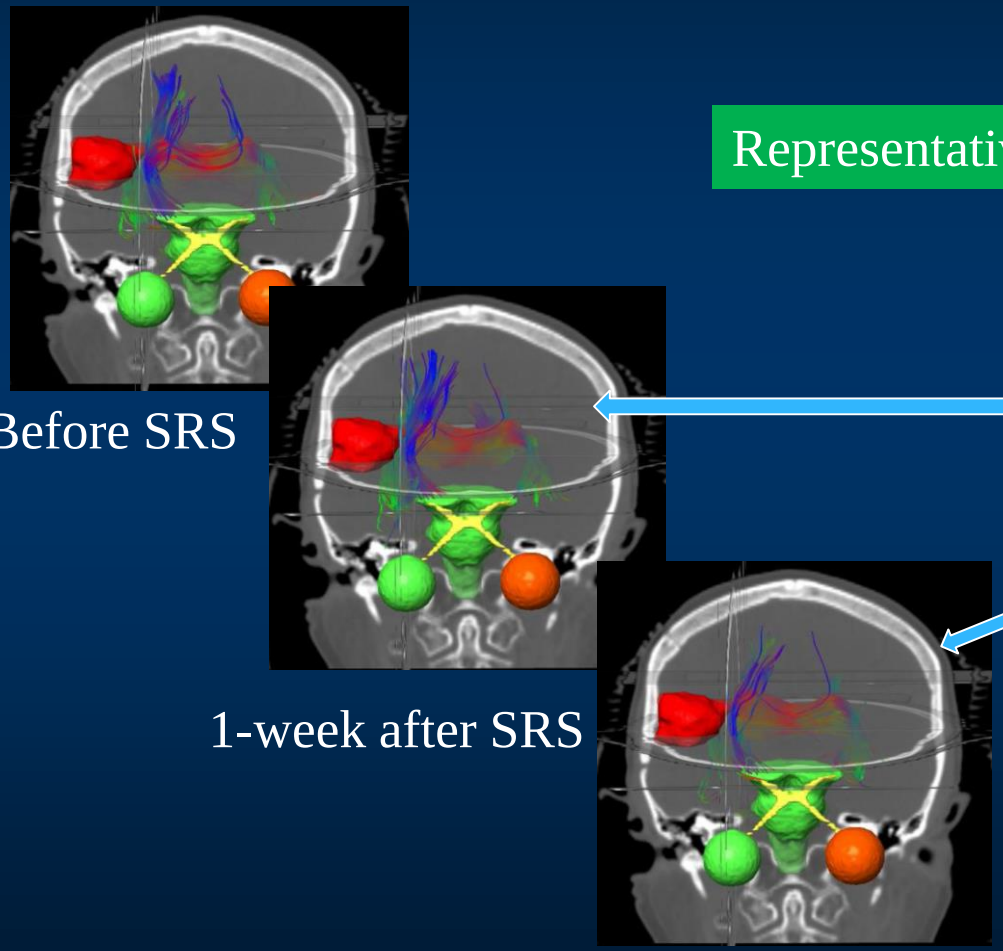

Before SRS

1-week after SRS

2-month after SRS

Representative Patient

Neural fibers decline

Chang Z, et al., Technol Cancer Res Treat, 2014.

Assessment using Diffusion MRI –White Matter Damage

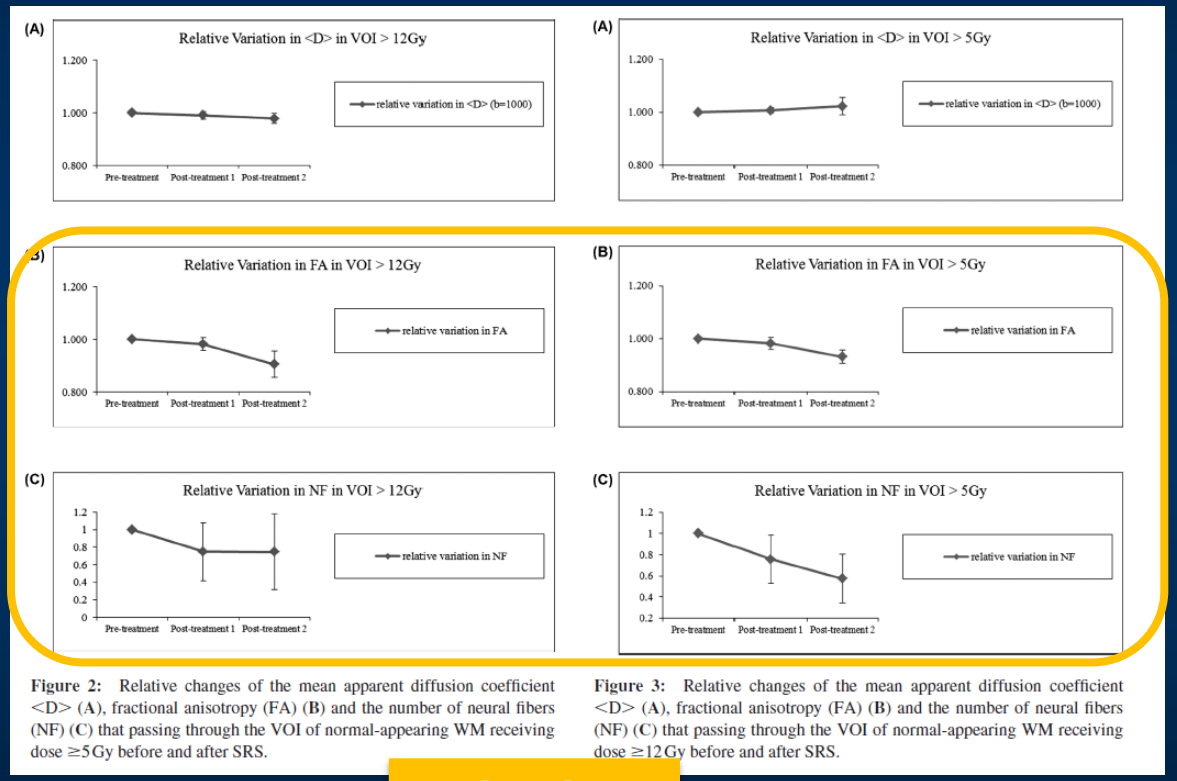

Figure 2: Relative changes of the mean apparent diffusion coefficient <D> (A), fractional anisotropy (FA) (B) and the number of neural fibers (NF) (C) that passing through the VOI of normal-appearing WM receiving dose ≥5Gy before and after SRS.

Figure 3: Relative changes of the mean apparent diffusion coefficient <D> (A), fractional anisotropy (FA) (B) and the number of neural fibers (NF) (C) that passing through the VOI of normal-appearing WM receiving dose ≥12Gy before and after SRS.

Irradiated area

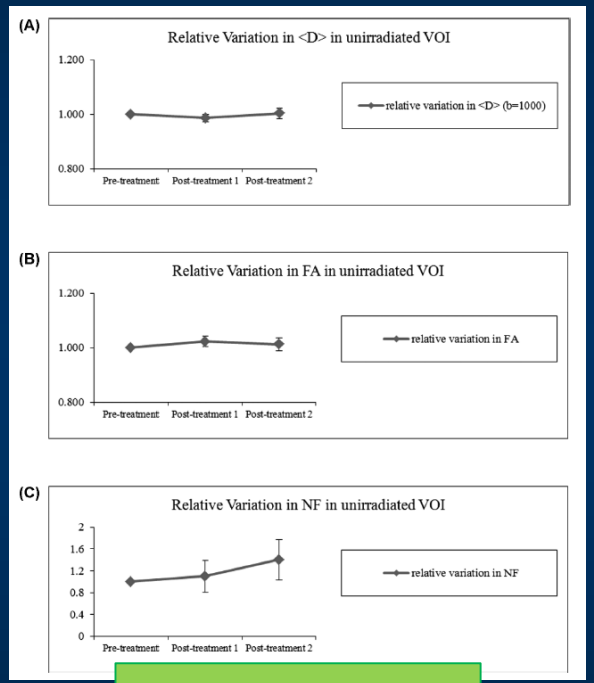

Non-irradiated contralateral area

FA decreased significantly by 6.8% ($p<0.01$) with nearly 40% ($p = 0.02$) decline of NF after two months of SRS in the VOIs of white matter receiving ≥ 5Gy

Chang Z, et al., Technol Cancer Res Treat, 2014.

Assessment using Diffusion MRI –White Matter Damage

- Stereotactic radiosurgery (SRS) has been an effective treatment for the management of brain metastases, acoustic neuromas and other brain diseases.
- Few data are available regarding radiation induced white matter (WM) damage by SRS.
- As compared with non-irradiated contralateral area, considerable decrease in fractional anisotropy (FA) and tracked neural fibers in the irradiated white matter volumes after 1-week of SRS, with further decrease after 2-month after SRS.

Chang Z, et al., Technol Cancer Res Treat, 2014.

Outline

- Introduction of MR quantitative imaging for treatment assessment
- Review of diffusion imaging, DCE/DSC imaging…
- Treatment assessment using diffusion MRI
- Treatment assessment using DCE-MRI
  - Assessment of tumor response –Brain
  - Assessment of radiation-induced normal tissue damage
- Developments of MR quantitative imaging for treatment assessment
- Challenges and future directions

Assessment using DCE-MRI –Brian SRS

- Stereotactic radiosurgery (SRS) has been an effective treatment for the management of brain metastases, acoustic neuromas and other brain diseases.
- A study of 12 patients with recurrent unifocal malignant gliomas, each up to 5 cm in maximum dimension.
- Patients were treated with concurrent SRS/BVZ treatment, with radiation dose of from 18Gy to 25Gy. Scanned 1-4 days prior to SRS and 7 days and two months after SRS treatment.
- Diffusion imaging and DCE-MRI were used to investigate for possible OS prediction.

Wang, et al., J. Radiosurgery and SBRT, 2018.

Results: Tumor Response

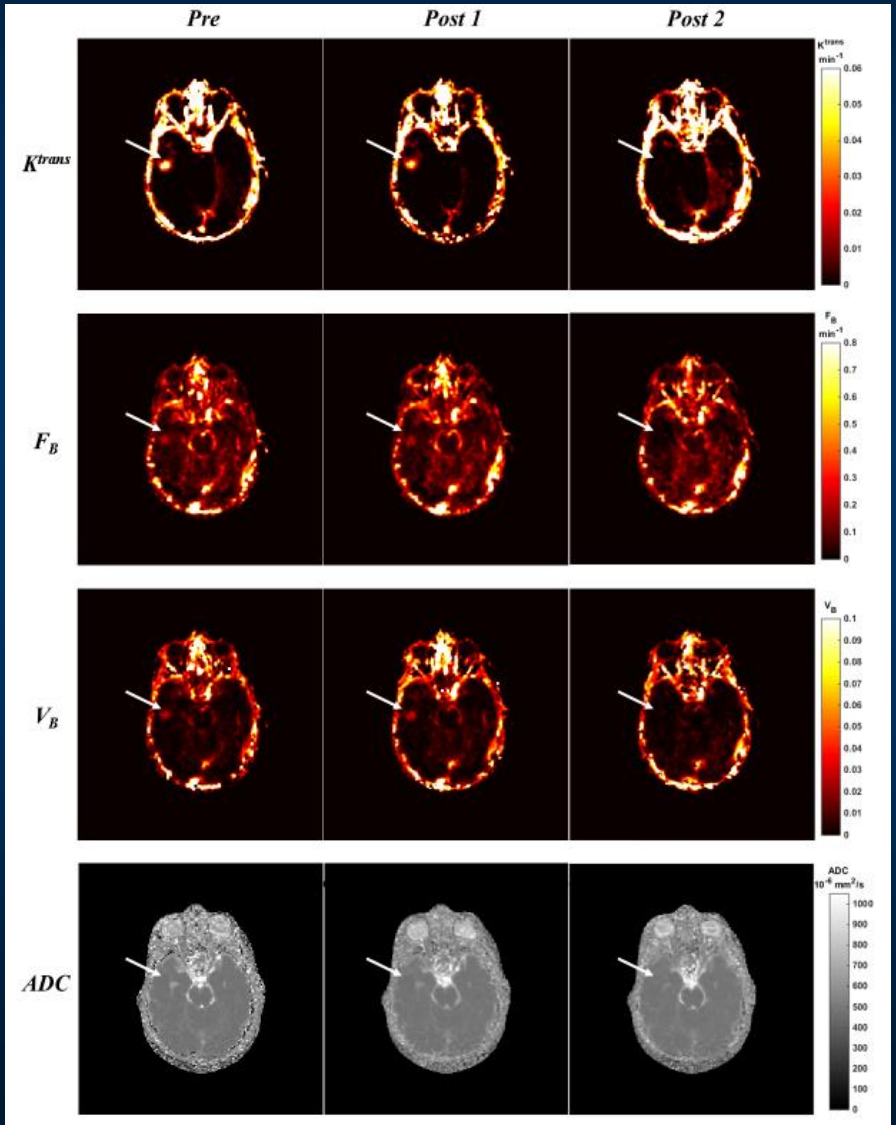

White arrows indicate the PTV location

Functional MR Parametric Maps from a selected patient.

Wang, et al., J. Radiosurgery and SBRT, 2018.

Results: Tumor Response

Summary of functional parameter statistics.

Para	ROI	*Pre scan*	*Post 1 scan*	*Post 2 scan*
K^{trans} min^{-1}	*PTV*	0.0183 ± 0.0115	0.0104 ± 0.0084	0.0030 ± 0.0054* (*p=0.035*)
	GTV	0.0196 ± 0.0155	0.0147 ± 0.0195	0.0064 ± 0.0033* (*p=0.035*)
	V12Gy – PTV	0.0100 ± 0.0068	0.0080 ± 0.0065	0.0058 ± 0.0091* (*p=0.035*)
		0.0084 ± 0.0055	0.0075 ± 0.0073	0.0065 ± 0.0080
F_B min^{-1}	PTV	0.0992 ± 0.0721	0.0687 ± 0.0581* (*p=0.017*)	0.0368 ± 0.0214* (*p=0.017*)
	GTV	0.0921 ± 0.0622	0.0680 ± 0.0565* (*p=0.017*)	0.0392 ± 0.0247* (*p=0.035*)
	V12Gy	0.0800 ± 0.0441	0.0682 ± 0.0481	0.0498 ± 0.0349
	V12Gy – PTV	0.0766 ± 0.0399	0.0685 ± 0.0456	0.0530 ± 0.0388
V_B	*PTV*	0.0127 ± 0.0093	0.0069 ± 0.0067	0.0034 ± 0.0022* (*p=0.017*)
	GTV	0.0117 ± 0.0087	0.0066 ± 0.0061	0.0037 ± 0.0028* (*p=0.035*)
	V12Gy – PTV	0.0100 ± 0.0072	0.0066 ± 0.0047	0.0056 ± 0.0052* (*p=0.035*)
		0.0095 ± 0.0070	0.0067 ± 0.0044	0.0062 ± 0.0060
ADC 10^{-6} mm^2/s	*PTV*	2664.4 ± 579.1	2704.8 ± 870.3	2609.3 ± 543.7
	GTV	2664.8 ± 514.8	2755.4 ± 752.5	2621.6 ± 558.0
	V12Gy – PTV	2749.1 ± 517.1	2794.4 ± 623.6	2744.1 ± 477.2
		2766.3 ± 550.0	2792.5 ± 603.4	2765.7 ± 463.0

Wang, et al., J. Radiosurgery and SBRT, 2018.

Radiomics

Intensity

#	Short	Feature Name
1	I -1	Energy
2	I -2	Entropy
3	I -3	Skewness
4	I -4	Kurtosis

Morphological

#	Short	Feature Name
5	M-1	Volume
6	M-2	Surface Area
7	M-3	Sphericity
8	M-4	Spherical Disproportion
9	M-5	Compactness 1
10	M-6	Compactness 2

Coarse Texture

#	Short	Feature Name
11	C-1	Short Run Emphasis
12	C-2	Long Run Emphasis
13	C-3	Gray Level Non-Uniformity
14	C-4	Run Length Non-Uniformity
15	C-5	Run Percentage
16	C-6	Low Gray Level Run Emphasis
17	C-7	High Gray Level Run Emphasis
18	C-8	Short Run Low Gray Level Emphasis
19	C-9	Short Run High Gray Level Emphasis
20	C-10	Long Run Low Gray Level Emphasis
21	C-11	Long Run High Gray Level Emphasis

Fine Texture

#	Short	Feature Name
22	F-1	Autocorrelation
23	F-2	Cluster Prominence
24	F-3	Cluster Shade
25	F-4	Cluster Tendency
26	F-5	Contrast
27	F-6	Correlation
28	F-7	Difference Entropy
29	F-8	Dissimilarity
30	F-9	GLCOM Energy
31	F-10	GLCOM Entropy
32	F-11	Homogeneity 1
33	F-12	Homogeneity 2
34	F-13	Informational Measure of Correlation 1
35	F-14	Informational Measure of Correlation 2
36	F-15	Inverse Difference Moment Normalized
37	F-16	Inverse Difference Normalized
38	F-17	Inverse Variance
39	F-18	Maximum Probability
40	F-19	Sum Average
41	F-20	Sum Entropy
42	F-21	Sum Variance
43	F-22	Variance

Wang, et al., J. Radiosurgery and SBRT, 2018.

Results: Radiomics

Normalized changes of radiomics features in different ROIs

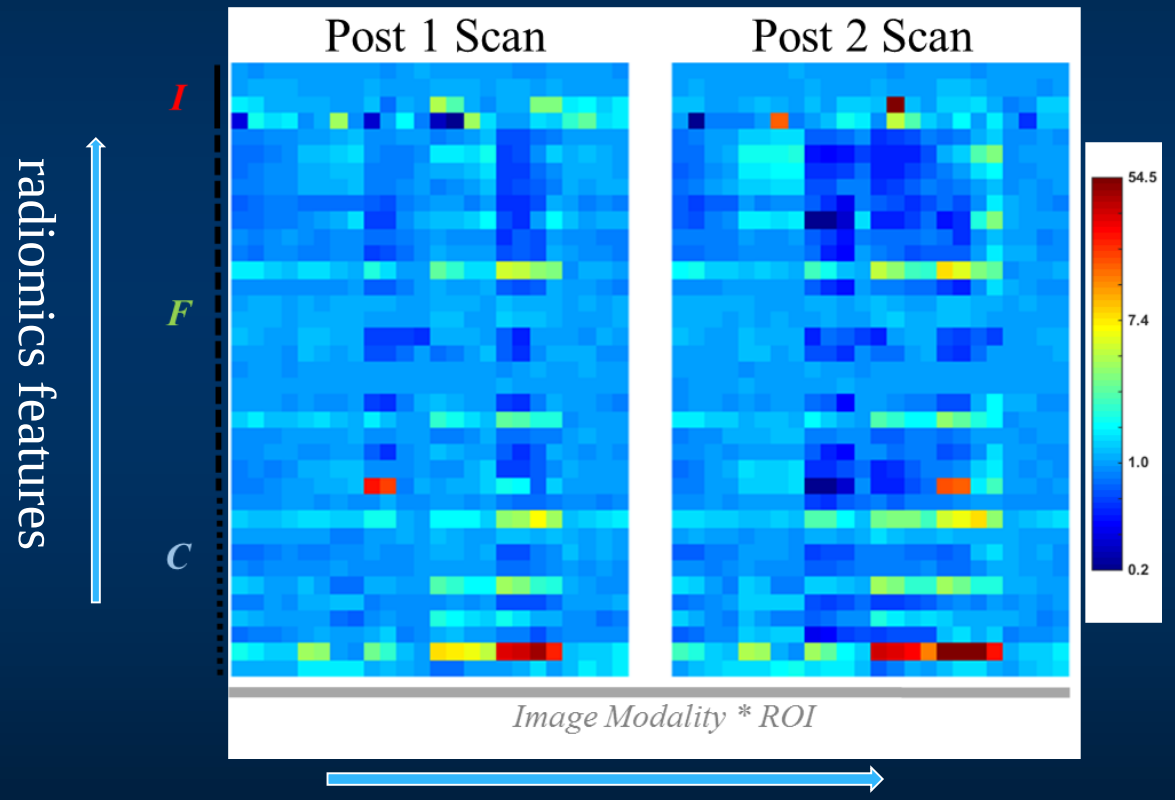

6 different image modalities in 4 different ROIs

Wang, et al., J. Radiosurgery and SBRT, 2018.

OS Prediction

- Selected radiomics features with high coefficient r values in correlation tests were investigated with support vector regression (SVR) to predict OS with leave-one-out cross validation.
- When using a selected group of 5 features' normalized changes (Ktrans: C-6 in PTV; ADC: C-7 in PTV; T1w: F-2 and C-7 in PTV; C-7 in GTV) in the 2nd post-treatment scan for outcome prediction, 9 out of 12 patients' OS time were accurately predicted (Mean absolute error = 1.47 mo, RMSE = 2.10 mo).

Wang, et al., J. Radiosurgery and SBRT, 2018.

Outline

- Introduction of MR quantitative imaging for treatment assessment
- Review of diffusion imaging, DCE/DSC imaging…
- Treatment assessment using diffusion MRI
- Treatment assessment using DCE-MRI
  - Assessment of tumor response –Brain
  - Assessment of radiation-induced normal tissue damage
- Developments of MR quantitative imaging for treatment assessment
- Challenges and future directions

Assessment using DCE-MRI– Neurocognitive Dysfunction

- Radiation therapy (RT) is a major treatment modality for malignant and benign brain tumors.
- The major limiting factor in its use is neurotoxicity, often as late neurocognitive dysfunctions.
- Important to identify biomarkers (e.g. cerebral vascular injury) for early assessment and prediction of late neurotoxicity…
- A study of 10 patients with low-grade glioma or benign tumor, treated with 3D conformal RT, with radiation dose of 50.4–59.4 Gy in 1.8 Gy fractions. 1–2 weeks prior to RT, at weeks 2–3 and weeks 5–6 during the course of RT, and at 1 month and 6 months following the completion of RT.

Cao, et al., Clin Cancer Res. 2009

Assessment using DCE-MRI– Neurocognitive Dysfunction

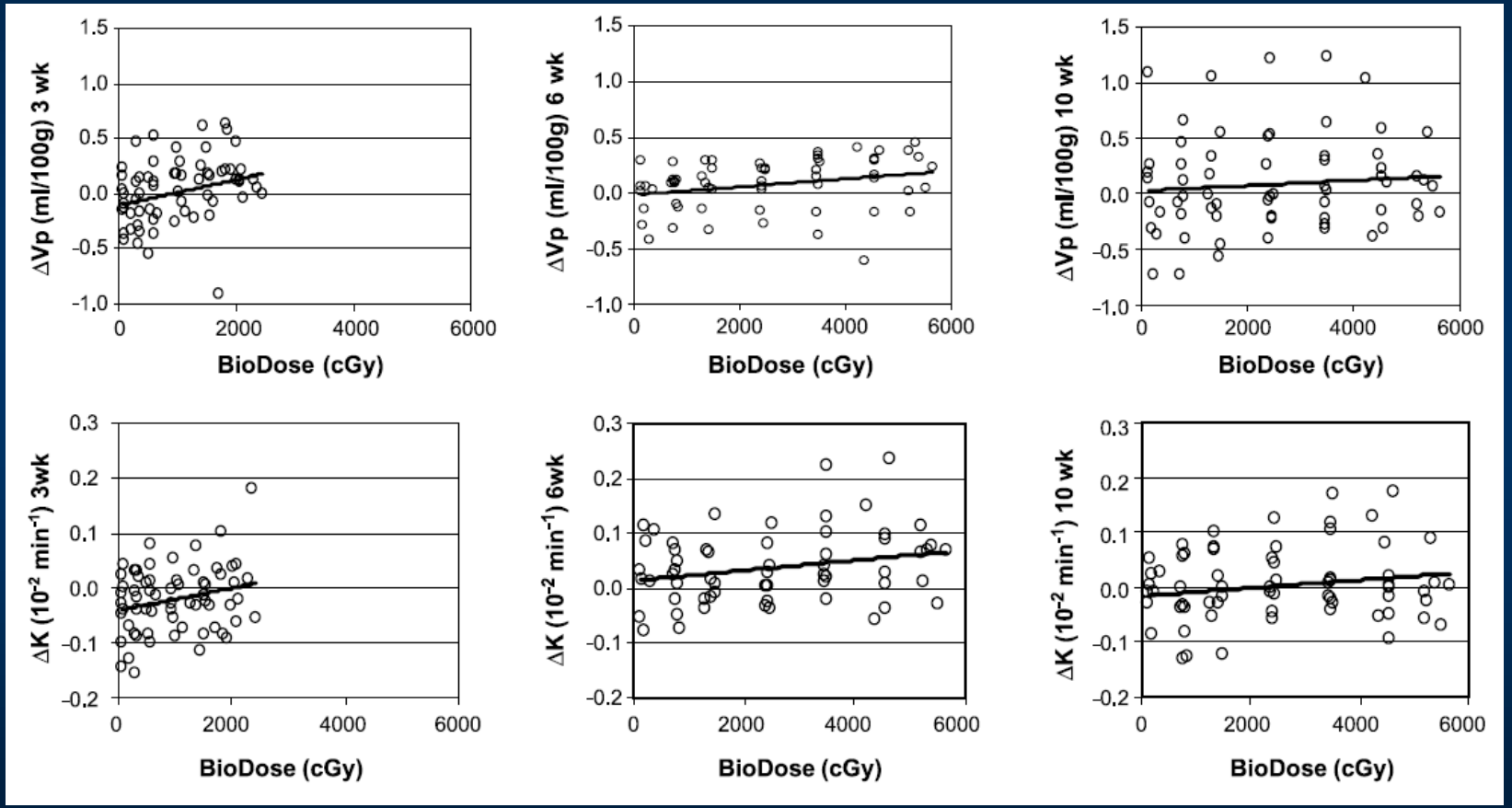

Changes in vascular volumes (Vp) & blood-brain permeability (Ktrans) versus doses

Cao, et al., Clin Cancer Res. 2009

Assessment using DCE-MRI– Neurocognitive Dysfunction

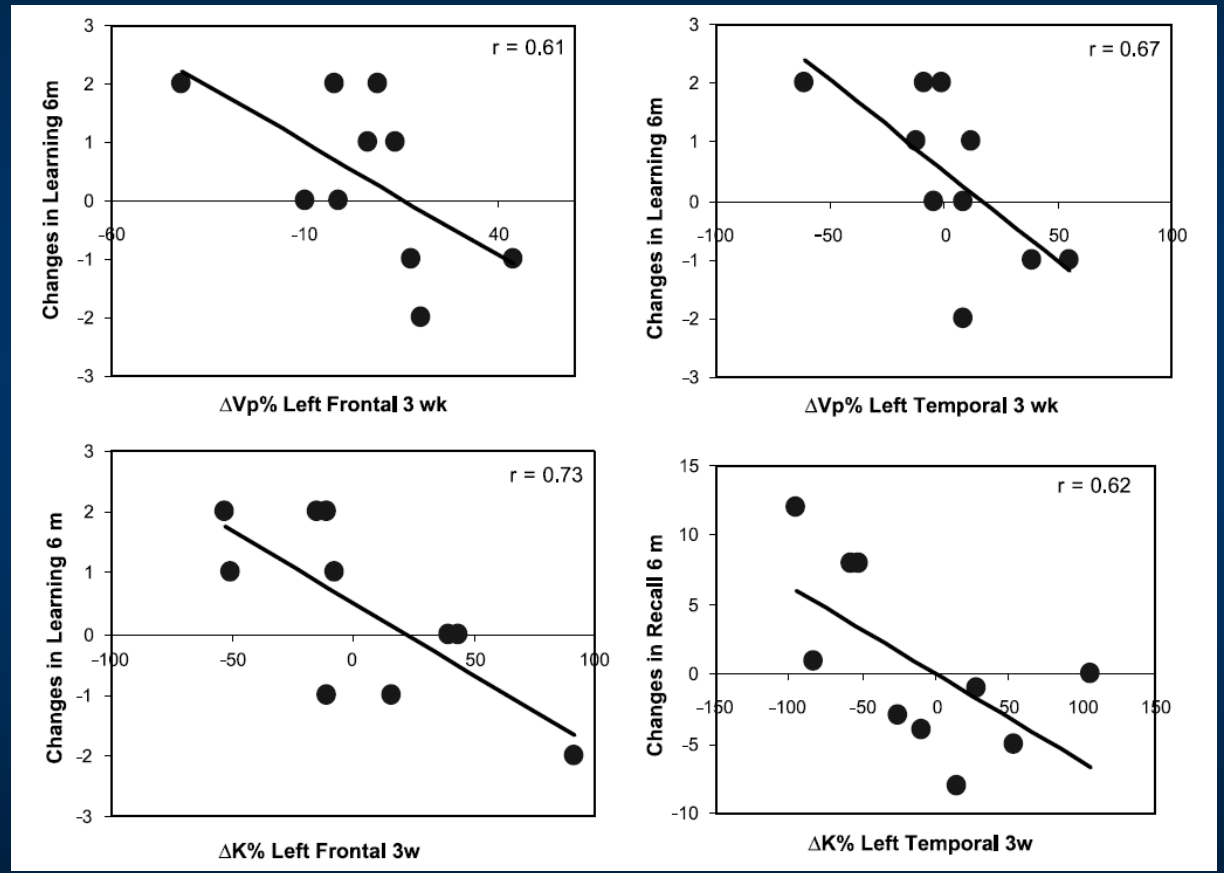

Learning scores decline as changes in Ktrasn and Vp

Cao, et al., Clin Cancer Res. 2009

Challenges and Limitations

Various technical challenges and limits encountered:

- Artifacts: distortions, motion artifacts ….
- Long data processing for PK analysis in DCE-MRI
- Relatively low temporal resolution in DCE-MRI
- ……

Outline

- Introduction of MR quantitative imaging for treatment assessment
- Review of diffusion imaging, DCE/DSC imaging…
- Treatment assessment using diffusion MRI
- Treatment assessment using DCE-MRI
- Developments of MR quantitative imaging for treatment assessment
- Challenges and future directions

Challenges and Limitations

Various technical challenges and limits encountered:

- Artifacts: distortions, motion artifacts ….
- Long data processing for PK analysis in DCE-MRI
- Relatively low temporal resolution in DCE-MRI
- ……

Distortion Correction for Diffusion MRI using EPI

- Spatial and intensity distortion in EPI images due to inhomogeneous static magnetic fields is a well-known phenomenon

  - Spatial distortion in SE and GRE EPI, and additionally signal loss in the latter, have restricted its use

  - Distortion is most pronounced in PE direction in EPI

  - Depends on applied magnetic field, magnetic susceptibilities within the subject, geometry of the subject, and its orientation

Holland et al., Neuroimage. 2010

Distortion Correction for Diffusion MRI using EPI

- Distortions in EPI-based Diffusion MRI: Eddy-currents and EPI distortions

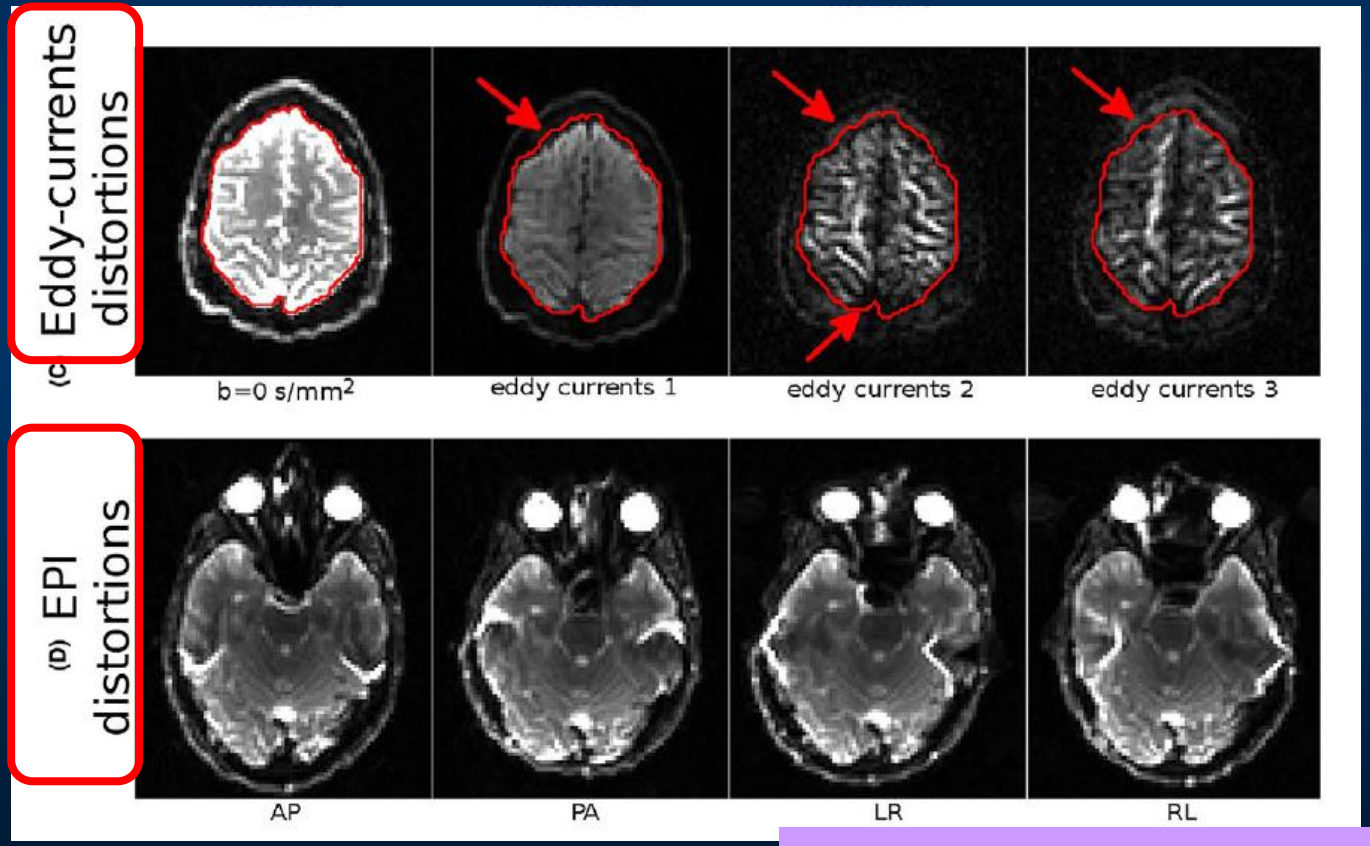

affect DWIs

affect DWIs, including the $b = 0$ s/mm^2

Irfanoglu et al., MRM. 2019

Distortion Correction for Diffusion MRI using EPI

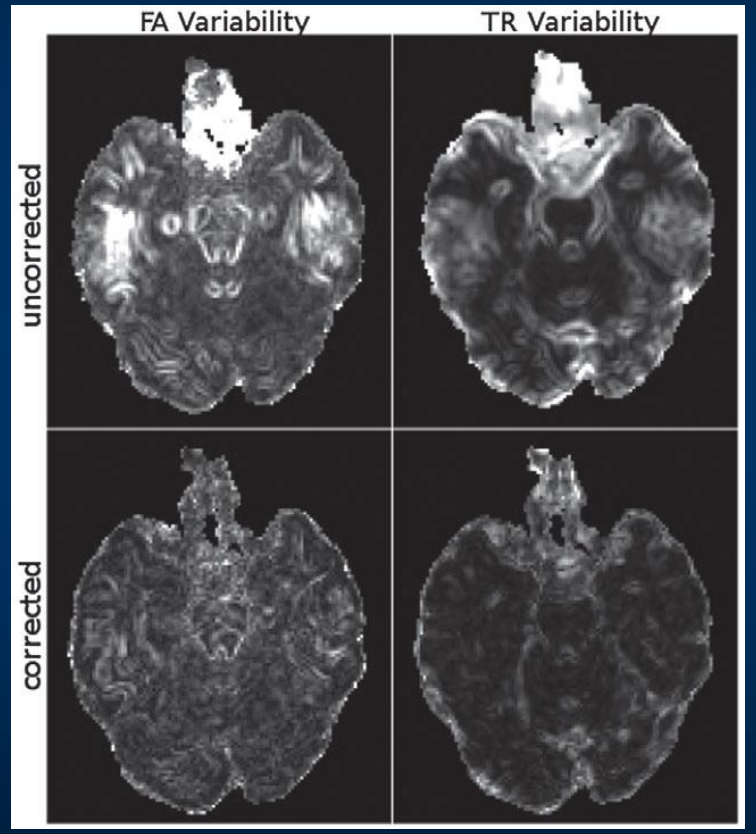

FA increase by 113% due to distortion

TR (trace) increase by 69% due to distortion

Irfanoglu et al., MRM. 2019

Distortion Correction for Diffusion MRI using EPI

- Spatial and intensity distortion in EPI images due to inhomogeneous static magnetic fields is a well-known phenomenon

  - Spatial distortion in SE and GRE EPI, and additionally signal loss in the latter

  - Distortion is most pronounced in PE direction in EPI

  - Depends on applied magnetic field, magnetic susceptibilities within the subject, geometry of the subject, and its orientation

- Various distortion correction methods have been proposed: the unwarping methods, PLACE, the reversed gradient methods

Holland et al., Neuroimage. 2010

Distortion Correction for Diffusion MRI using EPI

- The reversed gradient method makes use of the fact that the distortion behaves “symmetrically” when reversing the phase encoding direction

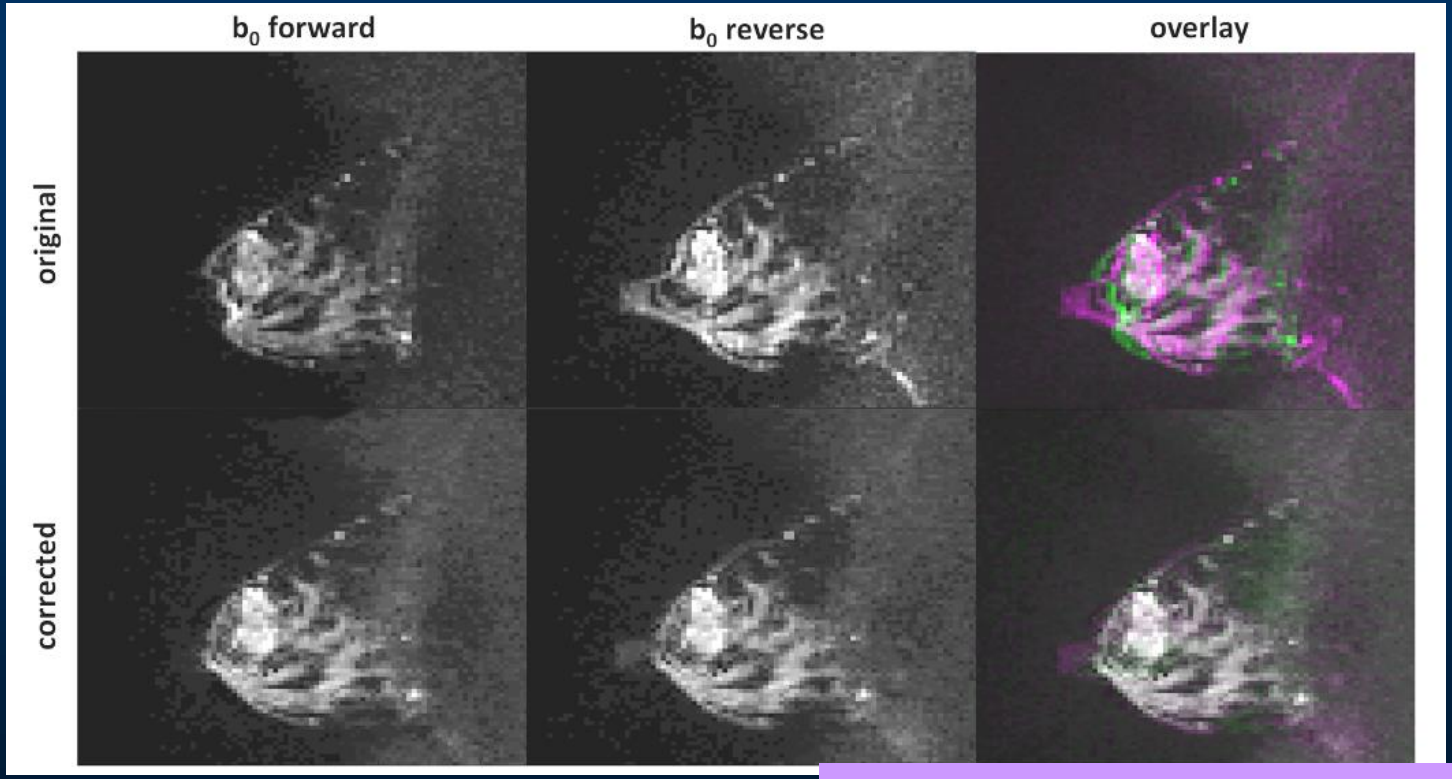

Teruel et al., MRM. 2015

Distortion Correction for Diffusion MRI using EPI

- Evaluating the correction strategies is challenging
  - Computer simulation,
  - Hardware phantoms,
  - Undistorted image (e.g. T1Wimage)
  - Framework based on the reversed PE and gradient methods

AP PE ← 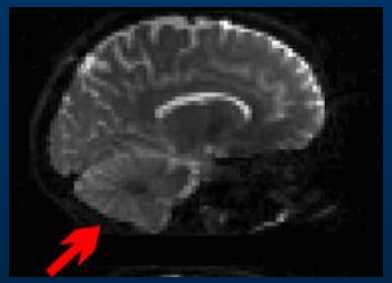 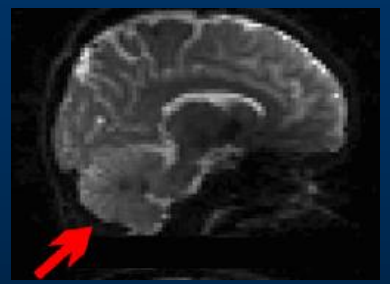 → PA PE

A perfect distortion correction method to the two datasets with opposite diffusion encoding directions or PE directions would produce identical images.

Irfanoglu et al., MRM. 2019

Distortion Correction for Diffusion MRI using EPI

- Evaluating the correction strategies is challenging
  - Framework based on the reversed gradient methods

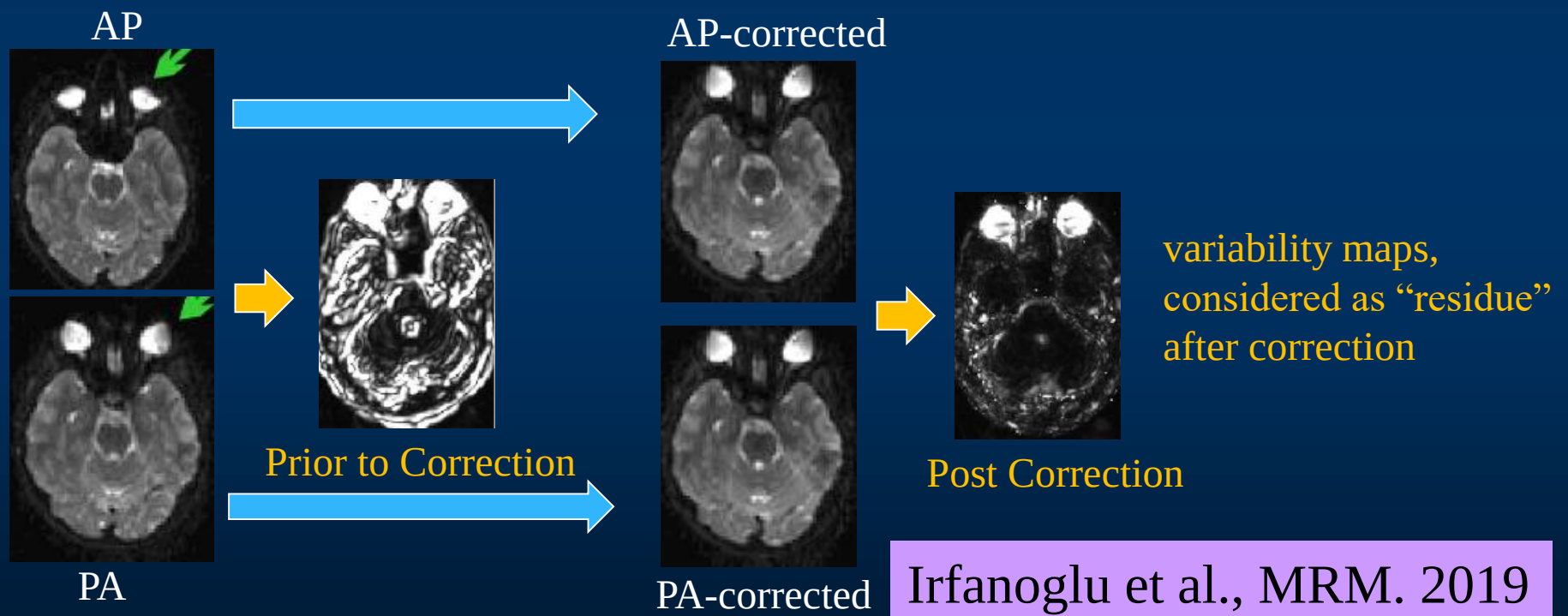

Irfanoglu et al., MRM. 2019

Froeling et al., MRM. 2017

Challenges and Limitations

Various technical challenges and limits encountered:

- Artifacts: distortions, motion artifacts ….
- Long data processing for PK analysis in DCE-MRI
- Relatively low temporal resolution in DCE-MRI
- ……

Efficient Calc. for DCE-MRI

- PK parameters in DCE-MRI analysis are commonly calculated with nonlinear least-squares (NLSQ) methods or linear least-squares method using the integral form of the PK model (ILLSQ)

  - NLSQ methods require intensive computation and may lead to erroneous results at the local optima

  - The computation time required for ILLSQ rapidly increases as temporal resolution of image acquisition increases

- Another efficient method for calculating pharmacokinetic (PK) parameters developed for DCE-MRI studies

Efficient Calc. for DCE-MRI

- To improve the computational efficiency, a new method for calculating PK parameters for DCE-MRI analysis was proposed.
- In this method, curve fitting based on linear least-squares method was applied to the derivative expression of the PK model with a KZ low-pass filter (abbreviated as the DLLSQ method).

$$C_t(t) = K^{trans} \int_0^t C_p(u) \cdot e^{-k_{ep}(t-u)}\, du + v_p \cdot C_p(t)$$

$$\frac{dC_t(t)}{dt} = (K^{trans} + v_p \cdot k_{ep}) \cdot C_p(t) - k_{ep} \cdot C_t(t) + v_p \cdot \frac{dC_p(t)}{dt}$$

2D simulation

K^{trans}

k_{ep}

v_p

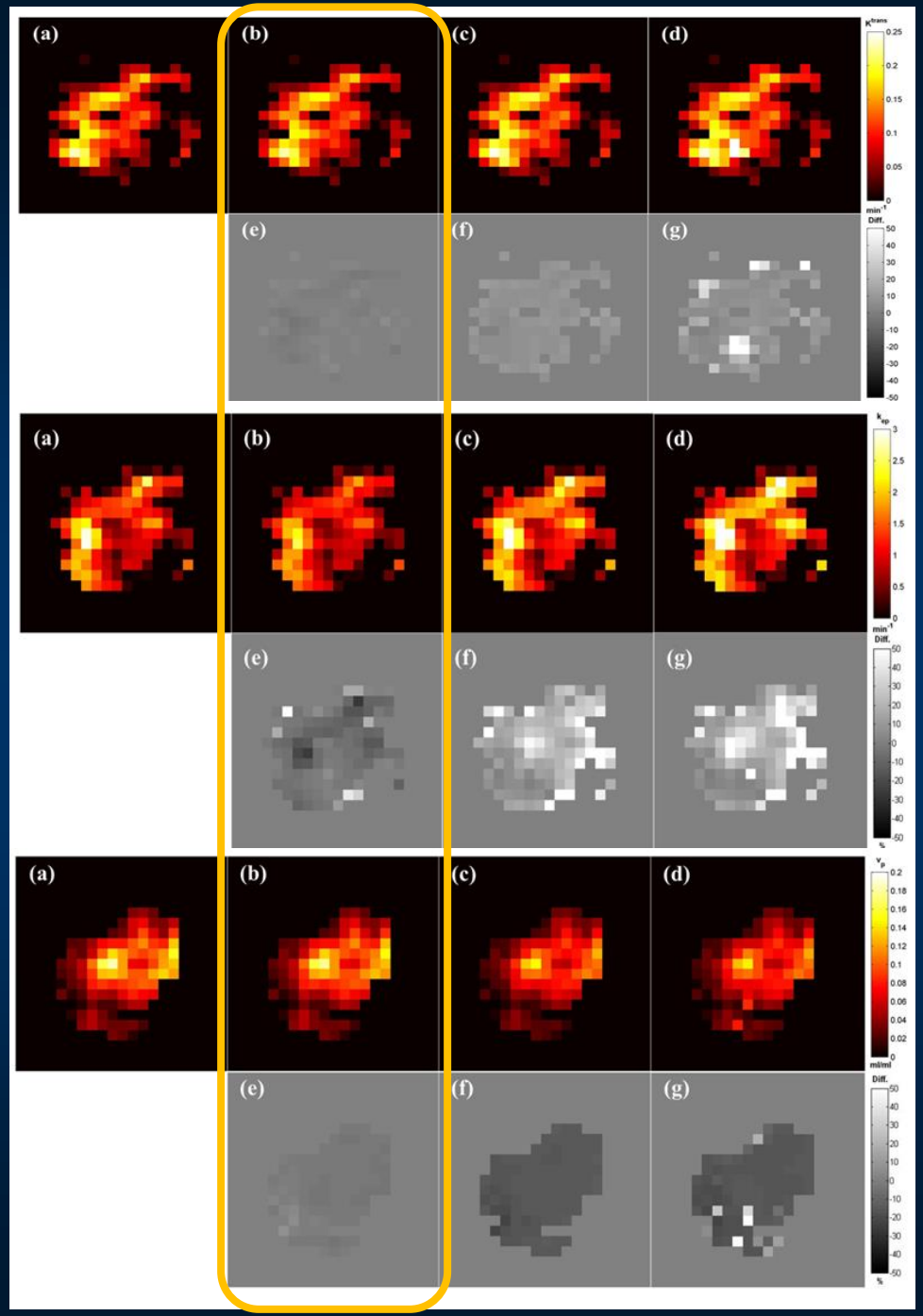

(a) True values;
(b) DLLSQ results;
(c) ILLSQ results;
(d) NLSQ results;
(e) difference map of DLLSQ results;
(f) difference map of ILLSQ results;
(g) difference map of NLSQ results

In vivo study

K^{trans}

k_{ep}

v_p

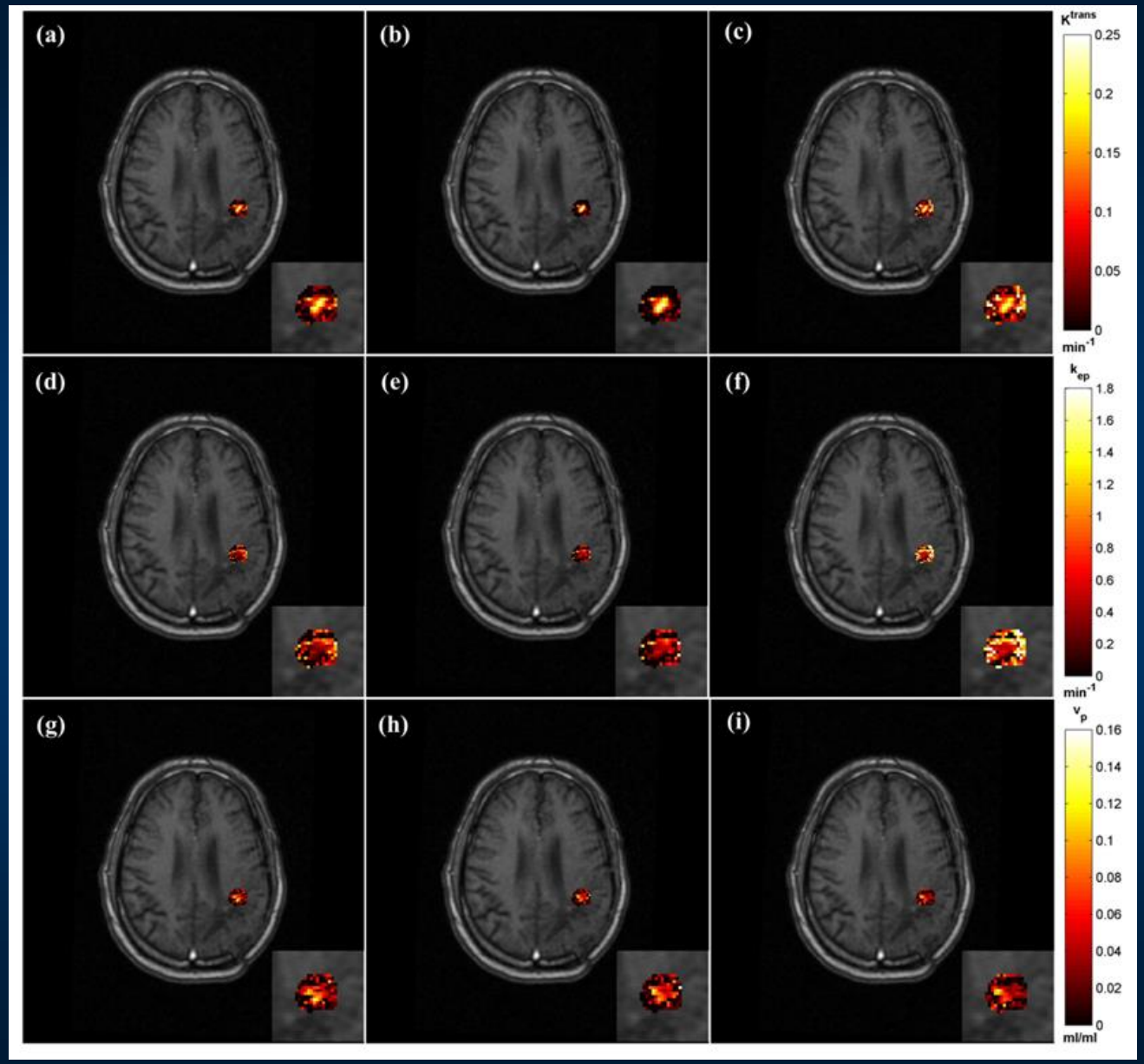

DLLSQ method ILLSQ method NLSQ method

Efficient Calc. for DCE-MRI

Δt(s)	0.1	0.5	1	2	3	4	5	10	15	20
DLLSQ	15.46	2.21	1.28	0.98	0.92	0.87	0.84	0.77	0.76	0.76
ILLSQ	$7.6x10^2$	32.90	9.31	3.21	2.06	1.63	1.41	1.09	1.02	1.00
NLSQ	2.86 $x10^4$	1.89 $x10^3$	$5.86x10^2$	$1.52x10^2$	82.53	52.17	31.96	13.04	13.86	12.40

In the simulation and *in vivo* studies, the calculated parameters using the proposed method were comparable to those using the existing methods with improved efficiency.

When analyzed within certain parameter intensity ranges at Δt=1s, the proposed method was more accurate than the current methods with improved efficiency by a factor up to 478.

C.Wang, FF. Yin, Z.Chang, MRM, 2015

Efficient Calc. for DCE-MRI using Deep Learning

- Machine learning (ML) based approach to directly estimate the PK parameters from the acquired DCE-MRI image-time series

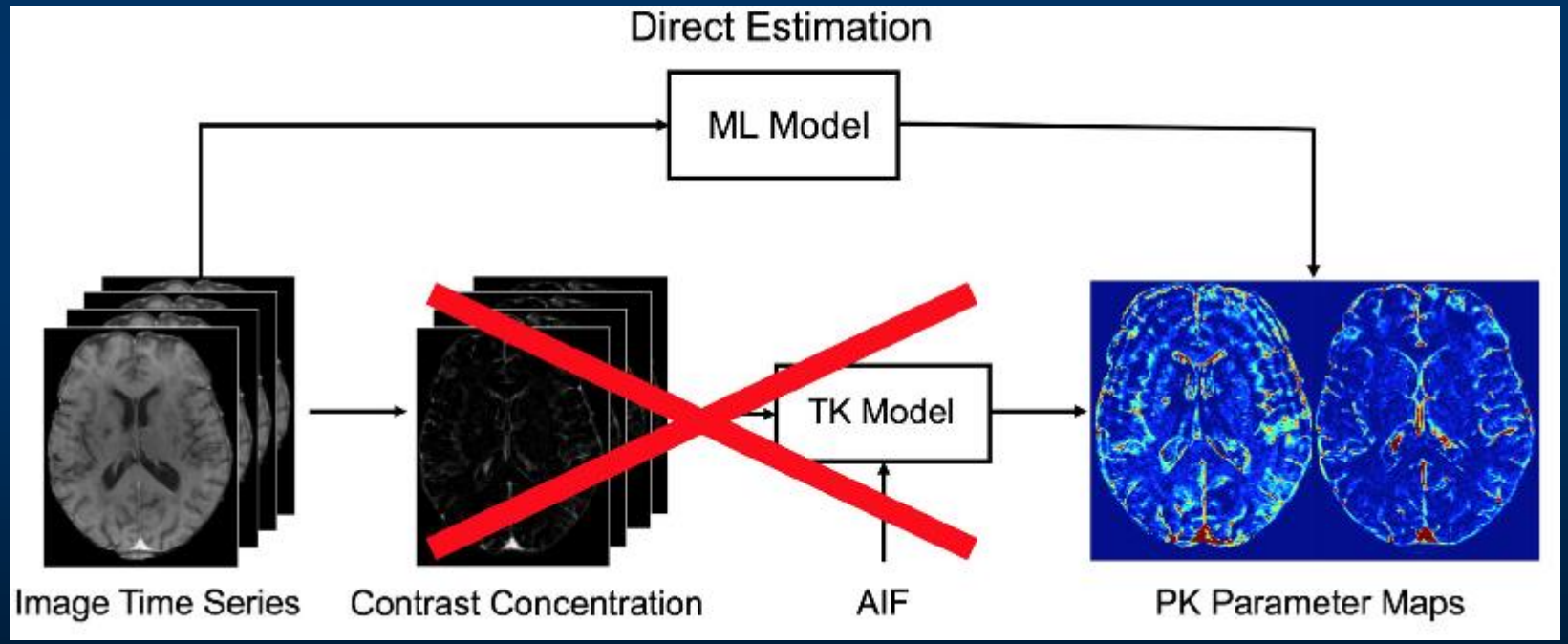

Ulas, et al,, Front Neurol. 2019

Efficient Calc. for DCE-MRI using Deep Learning

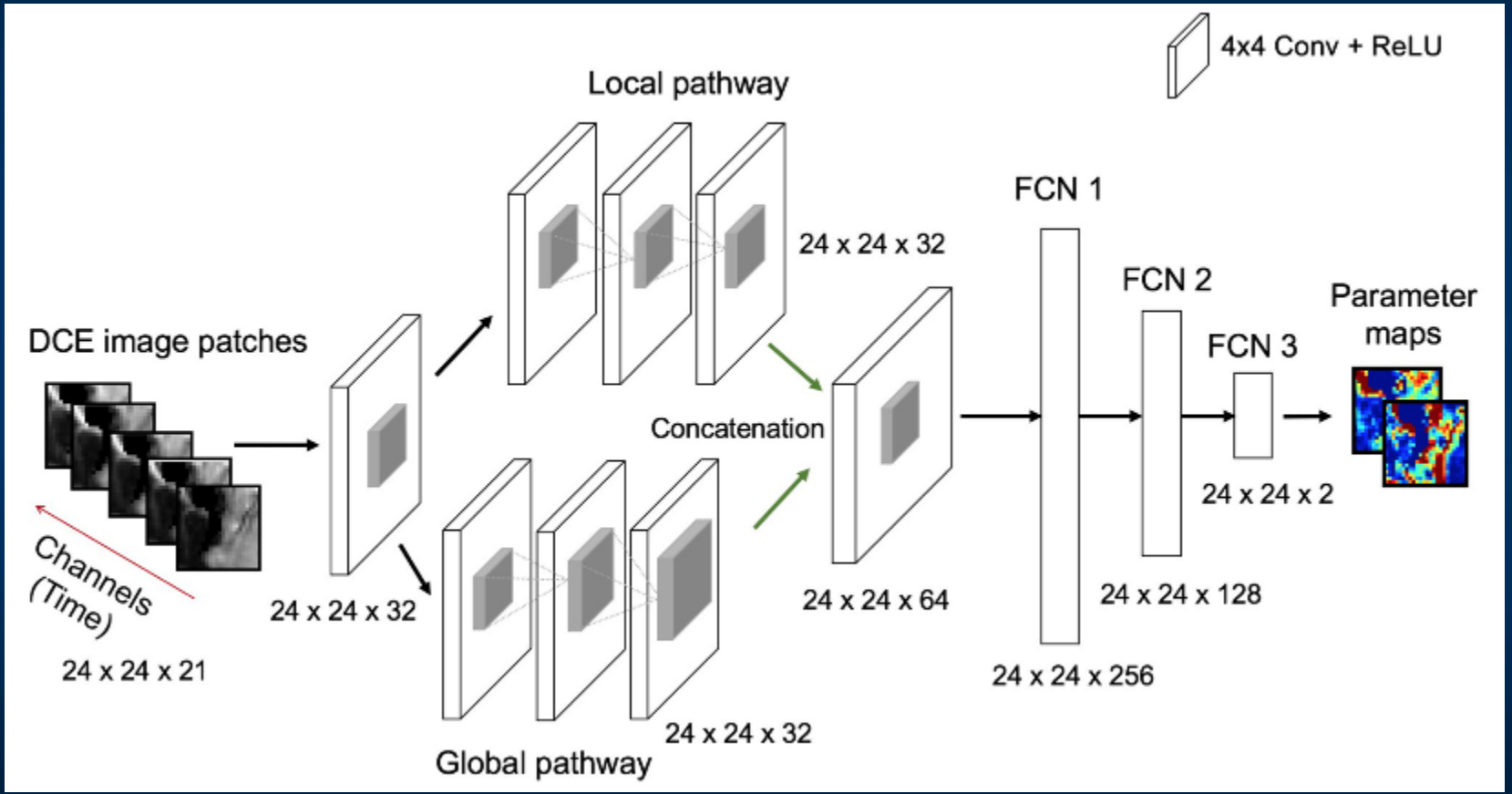

Over160 million training samples, i.e., number of total voxels, out of 15 patients

Deep Learning Architecture

Ulas, et al,, Front Neurol. 2019

Efficient Calc. for DCE-MRI using Deep Learning

- More robust and faster than conventional model fitting

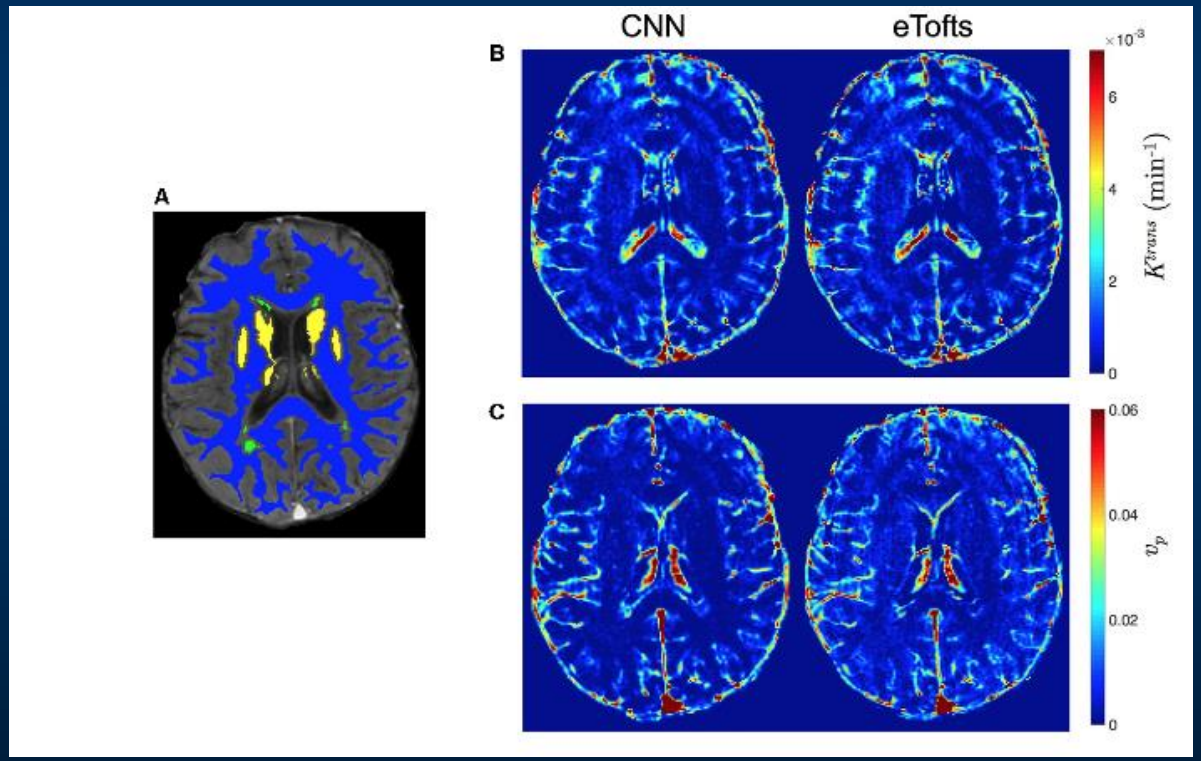

SSIM:0.998

SSIM: 0.961

A few seconds on a GPU machine

Ulas, et al,, Front Neurol. 2019

Challenges and Limitations

Various technical challenges and limits encountered:

- Artifacts: distortions, motion artifacts ….
- Long data processing for PK analysis in DCE-MRI
- Relatively low temporal resolution in DCE-MRI
- ……

Fast Imaging for DCE-MRI

High temporal resolution is desirable in DCE-MRI

- To ensure the accuracy of pharmacokinetics (PK) analysis

  Reliable AIF information derivation demands 1 s or faster

- To achieve feasible perfusion measurement

  Requires high temporal resolution to capture vascular phase of contrast medium delivery

Fast Imaging for DCE-MRI

To accelerate MRI acquisition, various fast imaging methods has been proposed

- Physically manipulate spin dynamics to use available magnetization more efficiently

  EPI, Spiral, RARE, GRASE, …

- Sparsely sample k-space and reconstruct a complete image through a non-standard reconstruction

  keyhole, SENSE, GRAPA, BLAST, SPEED, CS, TV,…

Fast Imaging for DCE-MRI

- Sparse radial sampled data can be reconstructed by using total variation (TV)/total generalized variation (TGV)
- The concept is based on the first order/second order derivative calculation was commonly adopted in the constrained image reconstruction as to minimize the gradient of the reconstructed image
- To explore the feasibility of fast DCE-MRI with TGV for tracer-kinetic (TK) studies

Fast Imaging for DCE-MRI

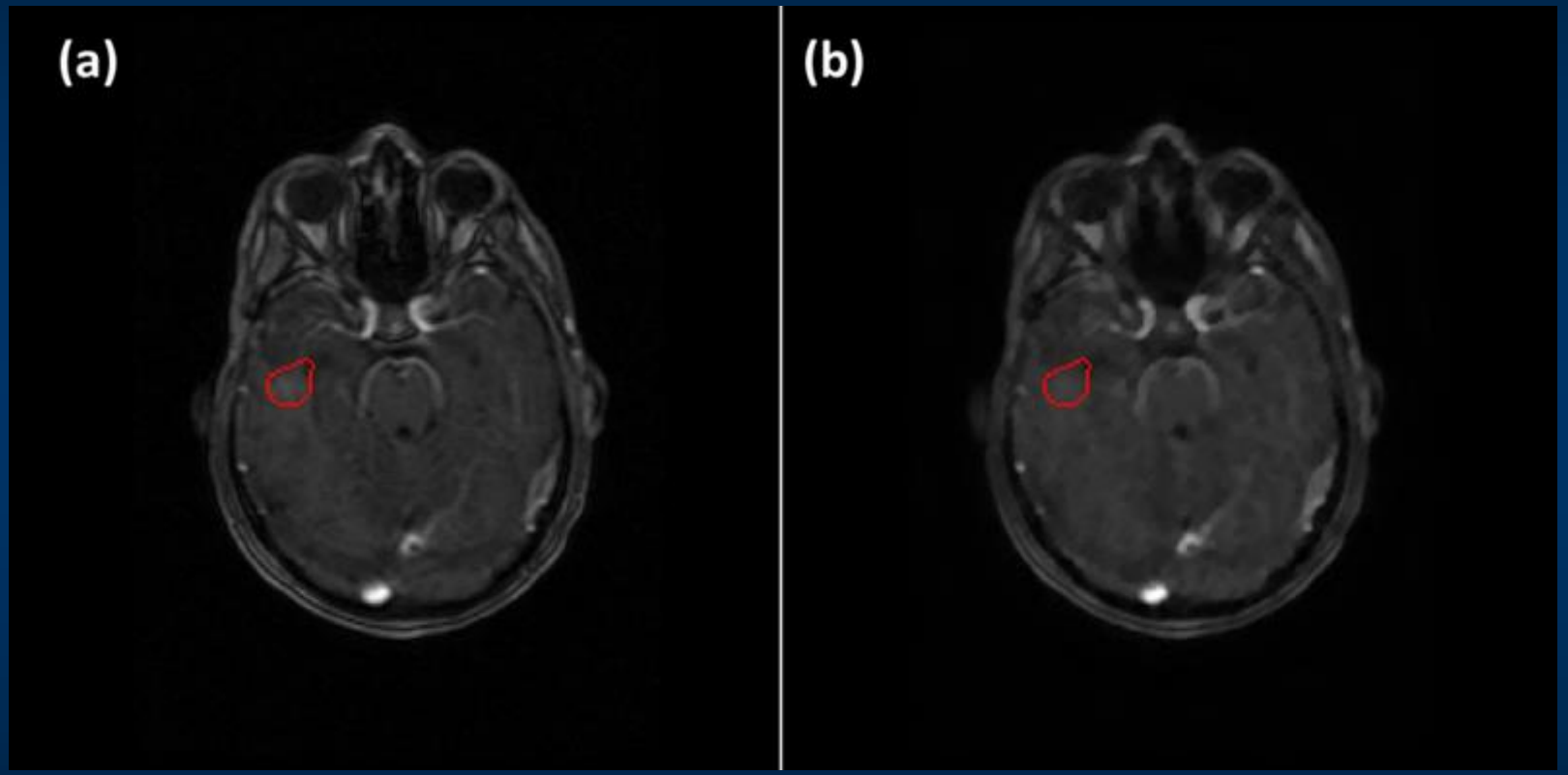

Original Reconstructed (x4)

Original post-injection image (a) and reconstructed image with 32 radial k-space lines(b). The red contour indicates ROI that contains the tumor

Fast Imaging for DCE-MRI

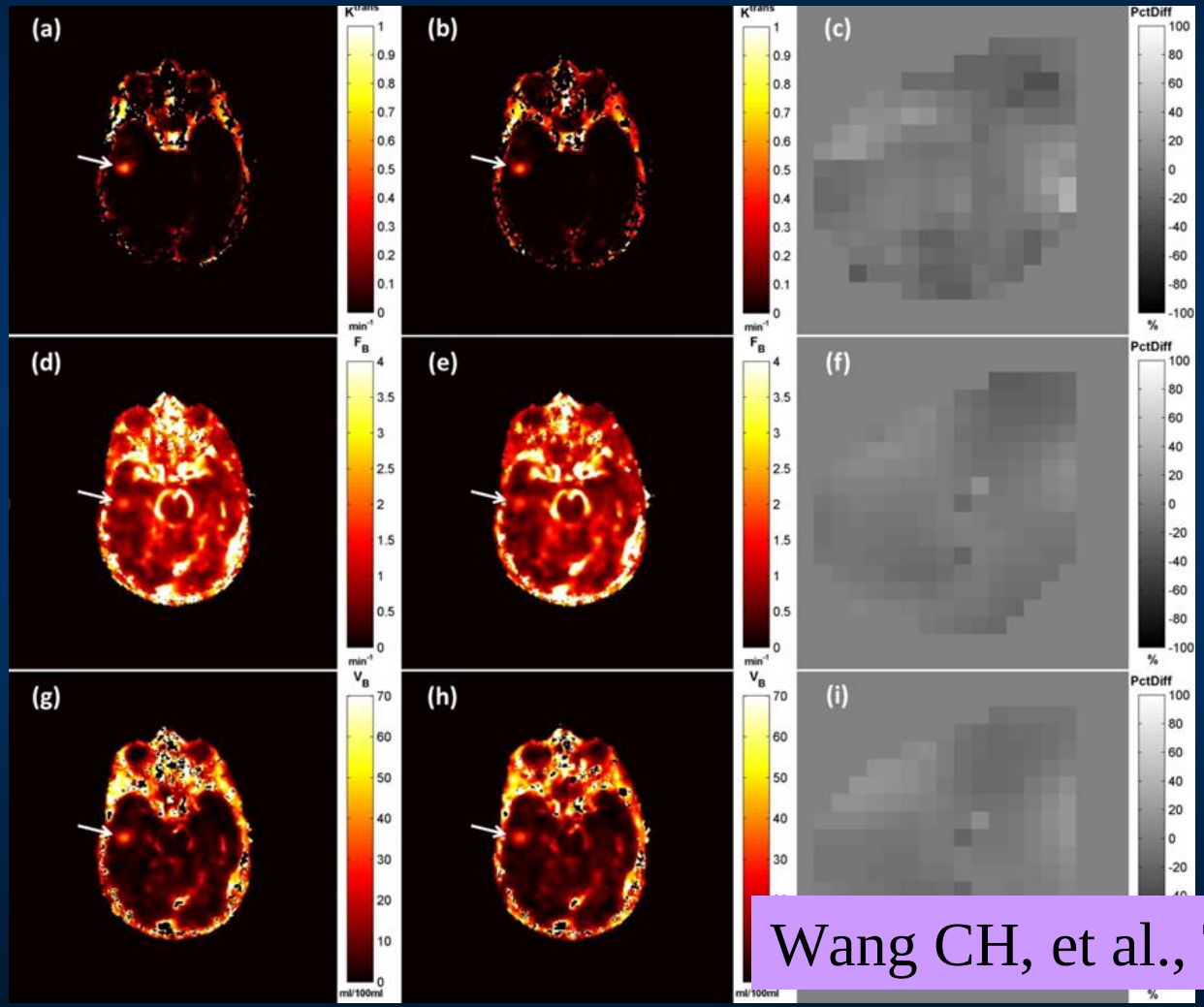

K^{trans} *Permeability*

F_B *Perfusion*

V_B *Perfusion*

Original Reconstructed (x4) Difference

Wang CH, et al., TCRT, 2016

Fast TK Mapping

- These techniques as “indirect” methods, because the anatomical image series are reconstructed first, followed by a separate step for TK parameter fitting
  - 1) Spatial TK parameter maps have much lower dimensionality than those of dynamic image series (two to four parameters, compared to 50–100 time points, per voxel), and
  - 2) TK model-based reconstruction directly exploits what is known about contrast agent kinetics
- “Direct” estimation of TK parameters from undersampled (k,t)-space data or undersampled DCE-MRI data

Fast TK Mapping

- These techniques as “indirect” methods, because the anatomical image series are reconstructed first, followed by a separate step for TK parameter fitting
- “Direct” estimation of TK parameters from undersampled (k,t)-space data or undersampled DCE-MRI data

Fast TK Mapping

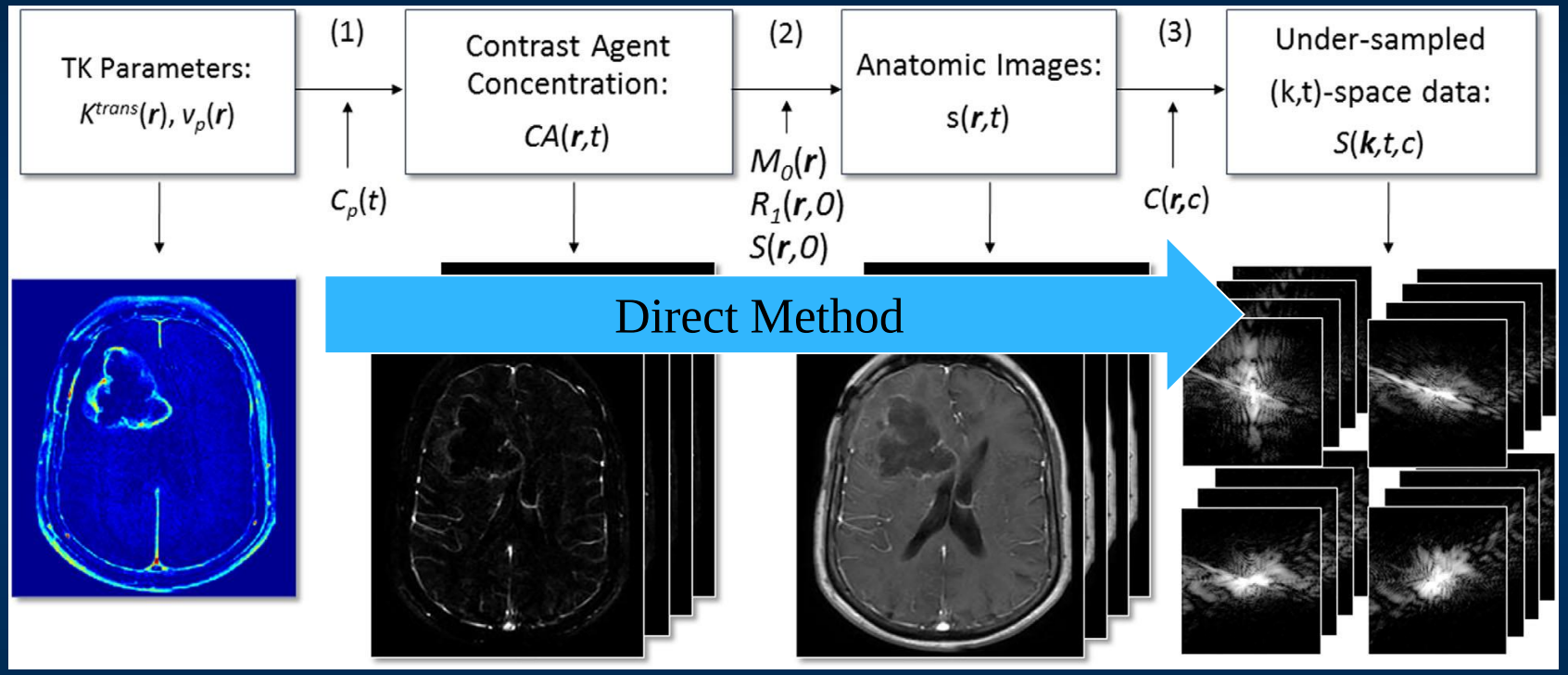

Y Guo, et al., MRM, 2017

DCE-MRI forward model flow chart:
Conversion from TK parameter maps to undersampled (k,t)-space.
Patlak model is used to convert TK parameter maps to contrast concentration

Fast TK Mapping

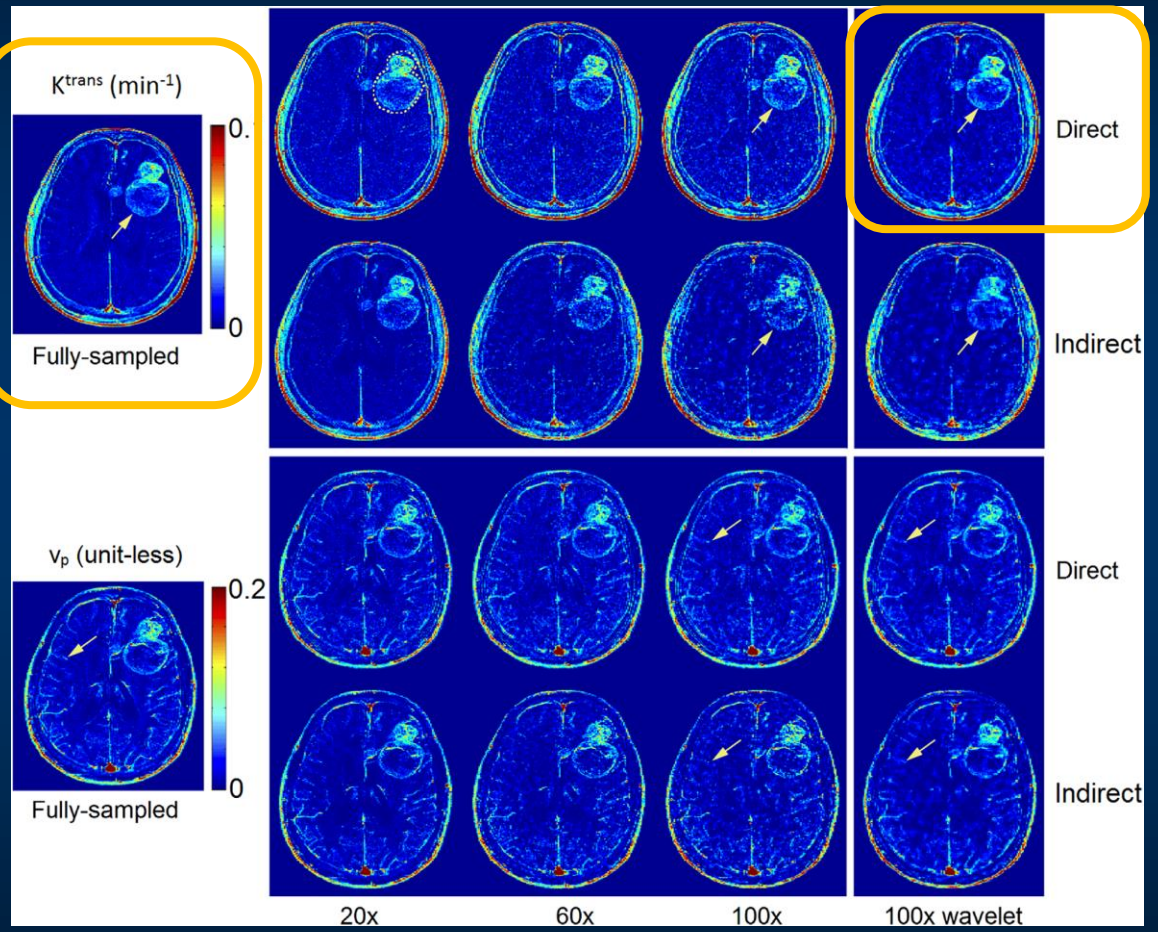

Retrospective evaluation of direct and indirect reconstruction of Ktrans and vp maps.

Ktrans map by Direct Method with the sparsity constraint

Undersampling rate:
R = 100

Only Patlak model used;
Use of more-sophisticated models (eg, extended Tofts model) possibly nonconvex, to be further investigated.

-Long computation time

Y Guo, et al., MRM, 2017

Fast TK Mapping

- These techniques as “indirect” methods, because the anatomical image series are reconstructed first, followed by a separate step for TK parameter fitting
- “Direct” estimation of TK parameters from undersampled (k,t)-space data or undersampled DCE-MRI data

Fast TK Mapping using Deep Learning

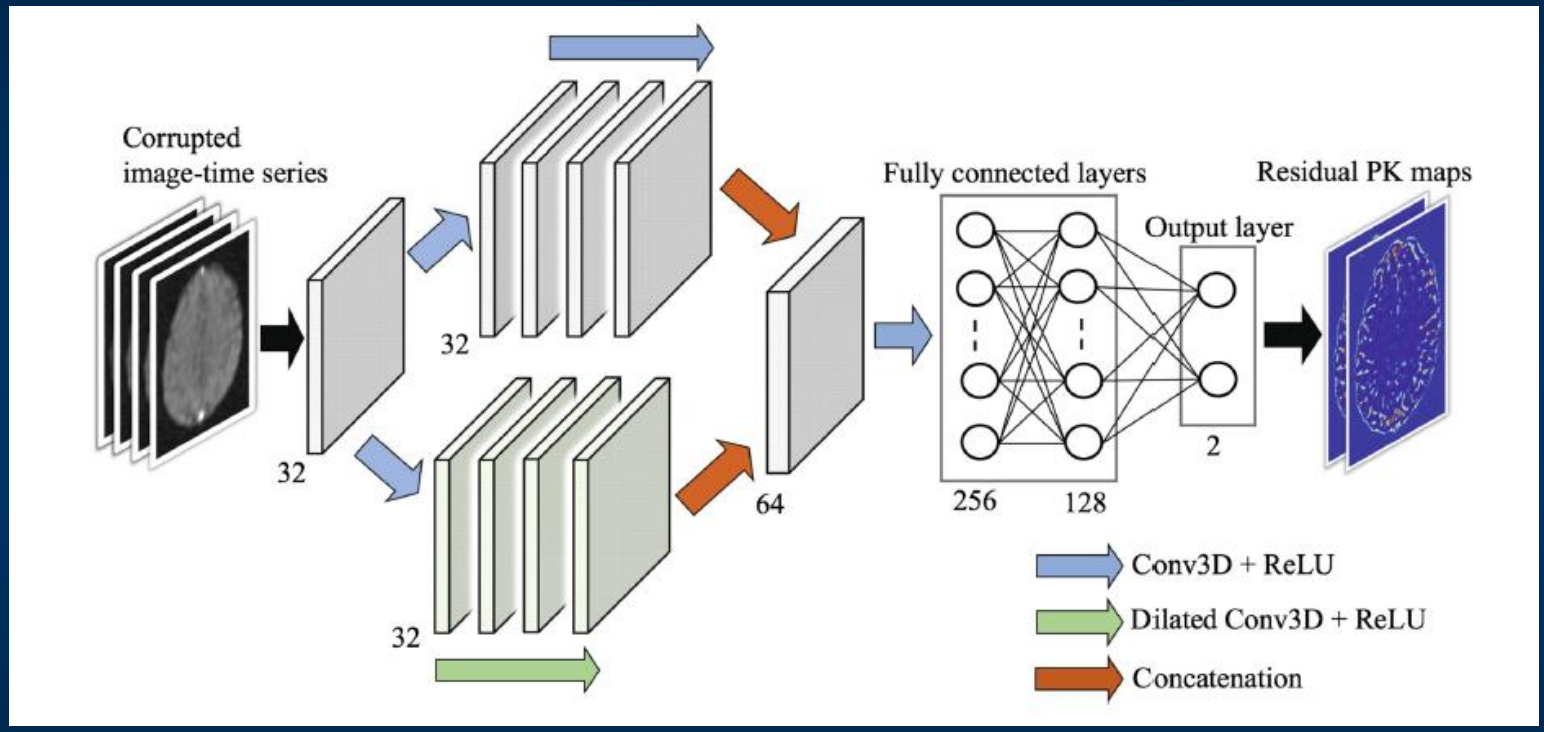

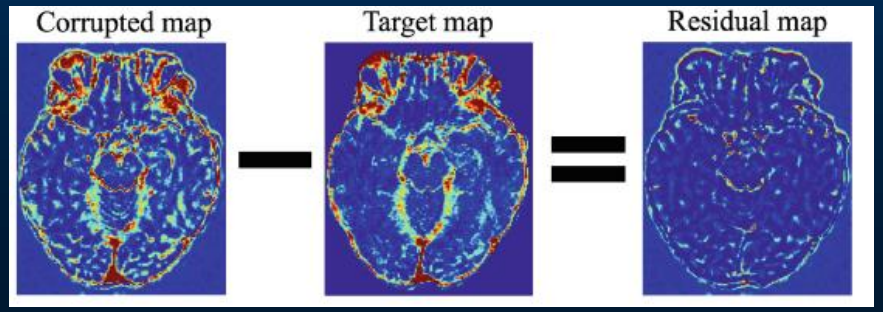

Deep Learning Architecture

Ulas, et al., MICCAI 2018

Fast TK Mapping using Deep Learning

Undersampling rate:
R = 10

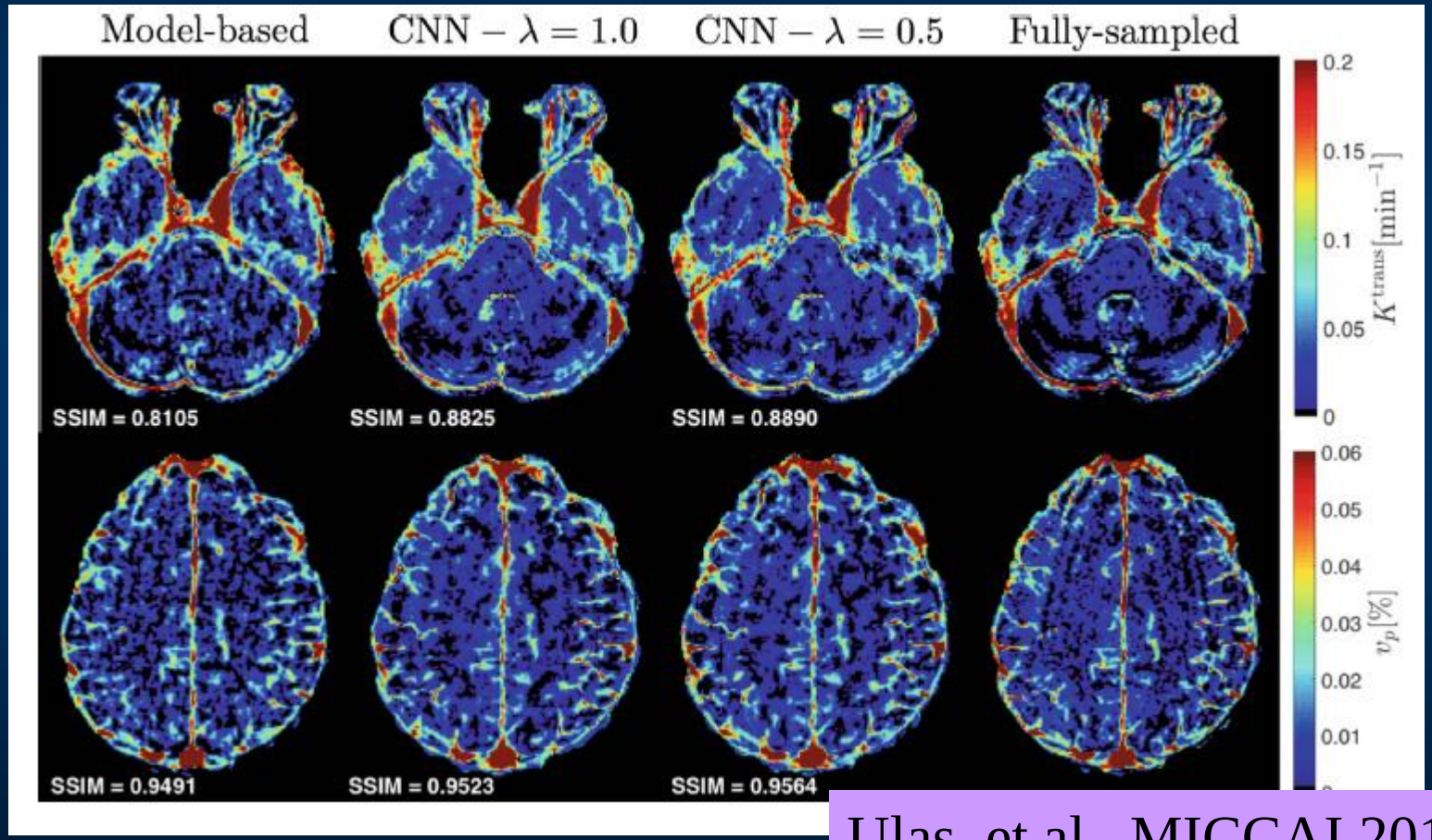

3D volume takes ~ 1.5 s for DL while the model-based direct method requires ~95 min

Ulas, et al., MICCAI 2018

Y Guo, et al., MRM, 2017

Outline

- Introduction of MR quantitative imaging for treatment assessment
- Review of diffusion imaging, DCE/DSC imaging…
- Treatment assessment using diffusion MRI
- Treatment assessment using DCE-MRI
- Developments of MR quantitative imaging for treatment assessment
- Challenges and future directions

Challenges and future directions

- Reproducibility of quantitative data

  To achieve this goal, standardized acquisition protocols, data analysis and assessment shall be promoted

- Interpretation of biomarker

  Physiologic meanings need to be fully examined towards the future clinical application

- Image quality improvement

  Potentially affect the quantitative assessment outcome

- Novel image analysis methodology

  Morphological information image texture features, deep machine learning

Z.Chang, et al. WJR, 2015

Acknowledgements

(Listed in alphabetic order)

Alvin Cabrera, MD
Chunhao Wang, PhD
Fang-Fang Yin, PhD
Janet K. Horton, MD
Junzo Chino, MD
Jing Cai, PhD
J. Kirkpatrick, MD, PhD
Oana Craciunescu, PhD
Sheridan Meltsner, PhD
Wenzheng Sun, PhD

…..

Duke RadOnc Team Work by Therapists, Dosimetrists, Physicists and Physicians !

Acknowledge the research funding support from Varian Medical Inc.

Thank you!